LUT UNIVERSITY
LUT School of Energy Systems
LUT Mechanical Engineering

Toni Leppänen

STRAIN GAUGE MEASUREMENTS AND FE-ANALYSIS OF TIMBER TRUCK'S TRAILER'S FRAME

Updated 10.5.2020

Examiners: Prof. D. Sc. (Tech.) Timo Björk
M.Sc. (Tech.) Antti Ahola

ABSTRACT

Lappeenranta University of Technology
LUT School of Energy Systems
LUT Mechanical Engineering

Toni Leppänen

Strain gauge measurements and fe-analysis of timber truck's trailer's frame

Master's thesis

2020

50 pages, 40 figures and 4 appendices

Examiners: Prof. D. Sc. (Tech.) Timo Björk
M.Sc. (Tech.) Antti Ahola

Keywords: Timber truck, strain gauge measurement, fatigue, 4R-method, FEA

The goal of this master's thesis was to define maximum global and local loadings in Jyki's timber truck's trailer frame. At first trailer's frame was analyzed by FEM in static situations which gave the locations for maximum stresses and strains. From these results measurement plan was made for strain gauge measurements. The plan included static, controlled and continuous measurements. Static and controlled measurements results were compared to FE-models and resulted dynamic multipliers for different loading cases. Continuous measurements resulted equivalent loads for each strain gauge for each road type.

Based on FE-models and measurement results the most critical weld joint was selected from trailer's frame. Jyki provided a test specimen from this weld from which weld toe radius and residual stresses were measured. A four-point bending test was designed for this test specimen which measured weld's lifetime. The specifications for the test were got from FE-models which also were used to design the pressing tool. With the result of the test true FAT-class was calculated.

Based on continuous measurements and measurements made to the test specimen weld joint's lifetime was calculated with 4R-method. This result was compared to Hot Spot calculation's result.

TIIVISTELMÄ

Lappeenrannan teknillinen yliopisto
LUT Energiajärjestelmät
LUT Kone

Toni Leppänen

Puutavara-auton perävaunun rungon venymäliuskamittaukset ja fe-analysointi

Diplomityö

2020

50 sivua, 40 kuvaa ja 4 liitettä

Tarkastajat: Professori Timo Björk
DI Antti Ahola

Hakusanat: Puutavara-auto, venymäliuskamittaus, väsyminen, 4R-menetelmä, FE-analyysi

Diplomityössä haluttiin selvittää Jykin puutavara-auton perävaunun suurimmat globaalit ja paikalliset kuormitukset käytön aikaisissa tilanteissa. Perävaunua tutkittiin ensin FE-mallilla staattisissa tilanteissa, joista saatiin paikallistettua suurimmat rasitukset. Näiden tulosten perusteella laadittiin tutkimussuunnitelma venymäliuska mittauksia varten. Mittaukset koostuivat staattisista tilanteista, kontrolloiduista ajoista ja pitkäaikaismittauksesta. Staattisilla ja kontrolloiduilla mittauksilla saatiin vertailu tuloksia FE-malleille ja dynaamiset kertoimet eri ajotilanteista. Vastaavasti pitkäaikaismittauksista saatiin ekvivalentit kuormitukset jokaiselle liuskalle ajetuille eri tietyypeille.

FE-malleihin ja mittaustuloksiin perustuen valittiin kriittisin hitsausliitos perävaunun rungosta. Tästä saatiin Jykiltä mittauksia vastaava mallikappale, josta mitattiin hitsausliitoksen reunaviivan pyöristyssäteet ja jäännösjännitykset. Tälle mallikappaleelle suunniteltiin nelipistetaivutuskoe, jossa mitattiin hitsausliitoksen elinikä sykleissä. Testiin tarvittavat mitta- ja voimatiedot saatiin FE-mallista, jonka avulla myös painintyökalu suunniteltiin. Testin tuloksella saatiin laskettua liitoksen todellinen FAT-luokka.

Pitkäaikaismittausten ja koekappaleelle suoritettujen mittausten perusteella kriittisimmälle hitsausliitokselle laskettiin elinikä 4R-menetelmällä. Tätä tulosta verrattiin Hot Spot-metodilla laskettuun vertailuarvoon.

ACKNOWLEDGEMENTS

Gratitude for Jyki Oy and especially Matti Kultala for this thesis topic, to Vesa Järvinen from Unisigma Oy for conducting the measurements, to Timo Björk for guidance from LUT and to Laboratory of steel structures for executing tests. And thanks to all whom have been involved in this journey to graduation.

Toni Leppänen

10.5.2020

TABLE OF CONTENTS

LIST OF SYMBOLS

E	Young's modulus [MPa]
k	Strain gauge factor
R	Resistance [Ωm]
r	Weld toe radius [mm]
t	Thickness of plate [mm]
V	Voltage [V]
ε	Strain [µm]
σ	Stress [MPa]
$\sigma_{0,4*t}$	Mean stress at 0.4 times plate thickness [MPa]
$\sigma_{0,5*t}$	Mean stress at 0.5 times plate thickness [MPa]
$\sigma_{1,4*t}$	Mean stress at 1.4 times plate thickness [MPa]
$\sigma_{1,5*t}$	Mean stress at 1.5 times plate thickness [MPa]
$\sigma_{1,9*t}$	Mean stress at 1.9 times plate thickness [MPa]
σ_b	Bending stress [MPa]
σ_{hs}	Hot Spot -stress [MPa]
$\Delta\sigma_k$	Effective notch stress [MPa]
σ_m	Membrane stress [MPa]
σ_{nl}	Non-linear stress [MPa]
σ_{res}	Residual stress [MPa]
$\Delta\sigma_{R,d}$	Liitoksen FAT-luokka [MPa]
ΔR	Change of resistance [Ωm]
C_{ref}	Fatigue capacity [MPa]
$K_{t,m}$	Membrane stress factor
$K_{t,b}$	Bending stress factor
N_f	Calculated lifetime [cycles]
m_{ref}	Slope of the reference curve
R_{local}	Local stress ratio
R_m	Tensile strength [MPa]

LIST OF ABBREVIATIONS

ENS	Effective notch stress
FAT	Fatigue resistance
FEM	Finite element method
FE-model	Finite element -model
S-N	Stress-cycles relation
SWT	Smith-Watson-Topper-method
IIW	International Institute of Welding

1 INTRODUCTION

Automotive industry's objective is to make the cars as light as possible and the same concerns timber trucks. The goal is to make transportation more fuel efficient in rate of cargo per truck and that's why timber trucks and trailers' structures are being optimized increasingly. Thus, higher strength steels are being used in the trailers' frames to get the most optimized geometry and decreased weight. That's why fatigue strength analyses and calculations are needed.

The maximum weight of truck increased from 60 t to 76 t since 1.10.2013 in Finland. This weight is possible with a truck that has nine axels, 25.25 m length, distance of 19.3 m between first and last axel and 65 % of the weight is distributed to axels that has paired tires. At the same time the maximum height of the truck increased from 4.2 m to 4.4 m. (6.6.2013/407) These changes decreases driving cycles to factories and thus fuel consumption per ton are also decreased.

1.1 Background and goal

Loading of timber truck's trailer's frames are not always measured (by strain gauges) in designing process thus actual affecting forces in real use are unknown. In this study these loading is being measured in critical locations in the frame with different test environments and loadings. Those forces can be used for the future redesigning purposes and FE-analyses. By 4R-method can be calculated fatigue life for the most critical location in the frame and this provides the information what kind of life expectations can be achieved.

1.2 Research problem and questions

The research problem in this thesis is to define affecting forces in the frame and compare results to FE-models' results. This problem leads to following questions:

- What are the critical locations and details in the frame?
- What kind of forces are affecting in typical use of the truck?
- Are the FEA results reliable in this application?
- What is the lifetime of the most critical details?

1.3 Limitations

This study is limited to define affecting forces in critical places by strain gauge measurements. In the FE-models' chassis and tires are simplified and focus is in the frame and its improvements. The fatigue strength calculation by 4R-method is used in the most critical place in the frame.

1.4 Research methods

For this study methods are finite element analysis (FEA), strain gauge measurements and fatigue analysis by 4R-method. For FEA is used Femap 11.4.1 with NX Nastran solver. FEA results are used in the strain gauge measurements planning process to define affecting forces and force types in measurement locations and for fatigue strength calculations. Affecting forces in FE-models are verified by comparing to the strain gauge measurements results.

2 THEORY

In this part is explained all used methods and calculations that are needed in the study. Calculations include fatigue life estimation by 4R-method and other used methods. Calculation examples are presented in the appendices.

2.1 Theory of strain gauge measurements

Strain gauges are used to measure deformations in the material, elongation or contraction. Deformations can be caused by external force, heat influence or internal forces due to welding or casting. Strains are generally used to determine mechanical stress values and directions in the examined test item. Stress calculation is based on Hooke's law in plane stress condition. (HBM 2018)

$$\sigma_x = \frac{E}{1-v^2}(\varepsilon_x + v\varepsilon_y) \quad (1)$$

$$\sigma_y = \frac{E}{1-v^2}(\varepsilon_y + v\varepsilon_x) \quad (2)$$

In equations (1) and (2) σ is stress value in x- or y-direction, ε is strain value in x- or y-direction, v is Poisson's ratio and E is young's modulus which describes the stress-strain relation depending of the material and thus young's modulus. In strain gauges plane stress condition is as extreme case where ε_y is 0. As the strain gauge is positioned to the surface there isn't a third stress normal to the plane. Thus, strain gauge is in axial stress condition which leads to simplified equation (3) that can be used. (HBM 2018)

$$\sigma = \varepsilon * E \quad (3)$$

There are multiple types of strain gauges for different type of measurements, but the most common strain gauge has grid shaped sensing element that is made of thin resistive metallic foil. This foil is between plastic and laminate film. Resistive metallic foil has its original resistance and it changes when elongated or contracted. (HBM 2018)

$$\frac{\Delta R}{R} = k * \varepsilon \tag{4}$$

In equation (4) ΔR is change of resistance, R is original resistance and k is proportional constant (gauge factor). Gauge factor depends on the material composition used in the strain gauge. (HBM 2018)

2.1.1 Wheatstone bridge

Wheatstone bridge is classical electric circuit which consists four resistors. The bridge configuration is shown in Figure 1.

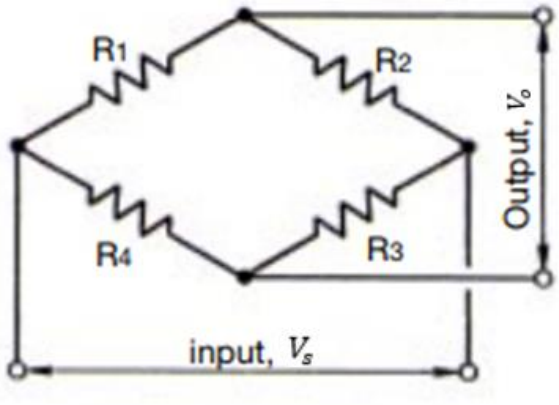

Figure 1. Wheatstone bridge configuration. (Kyowa 2014)

The bridge configuration is supplied with constant input voltage and output voltage is being measured. When the full bridge is imbalanced due to difference in the voltages it can be calculated as follows. (Kyowa 2014)

$$V_o = V_s * \left(\frac{R_1}{R_1 + R_2} - \frac{R_4}{R_3 + R_4}\right) \tag{5}$$

In equation (5) V_o is output voltage and V_s is input voltage. Then the original resistances in relation to resistance changes are inserted to the equation. (Kyowa 2014)

$$\frac{V_o}{V_s} = \frac{1}{4} * \left(\frac{\Delta R_1}{R_1} - \frac{\Delta R_2}{R_2} + \frac{\Delta R_3}{R_3} - \frac{\Delta R_4}{R_4}\right) \tag{6}$$

Next the resistance change relations are substituted by equation (4) strains times gauge factor. (Kyowa 2014)

$$\frac{V_o}{V_s} = \frac{k}{4} * (\varepsilon_1 - \varepsilon_2 + \varepsilon_3 - \varepsilon_4) \quad (7)$$

From equation (7) can be calculated strains as all the other variables are known. This equation represents full wheatstone bridge. Depending how many strain gauges are being used in this circuit it is called ¼-, ½- or full bridge. (Kyowa 2014)

2.2 Fatigue strength assessment of welded joints

When fatigue strength of welded joint is being assessed all types of varying loads needs to be taken account from different phases of life. These can be for example installation, transportation and in-service. From varying loads stress ranges or stress intensity factors ranges are calculated. Usually fatigue life assessment is based on one of these depending of the method being used. (Hobbacher 2014) Used methods are presented in this chapter.

2.2.1 Hot Spot-method

Structural stress σ_{hs} (hot spot stress) is an extrapolation method to define local stress in discontinuity (for example weld toe) or a situation where nominal stress isn't clearly defined due to complex geometrical effects. In these cases, notch stress is affecting which includes three components as figure 2 presents. (Hobbacher 2014)

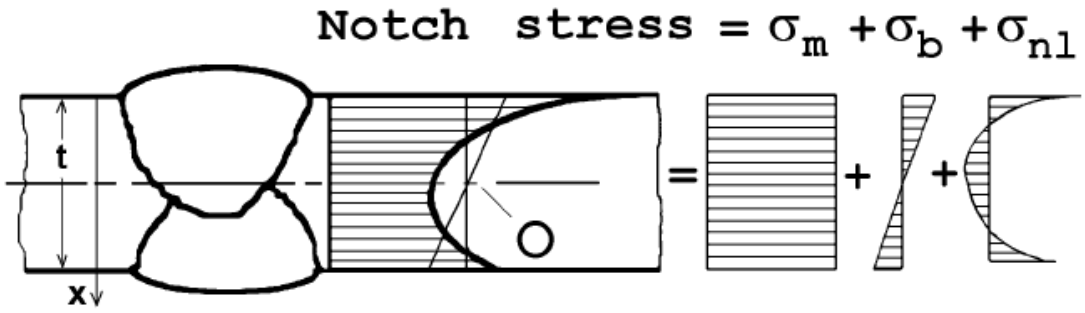

Figure 2. Notch stress components. (Hobbacher 2014)

In figure 3 σ_m is membrane stress, σ_b is shell bending stress and σ_{nl} is non-linear stress peak. Hot spot method excludes the non-linear stress peak by extrapolation where reference

points are used to determine stress at weld toe. As figure 3 shows this calculated extrapolation stress is structural stress. (Hobbacher 2014)

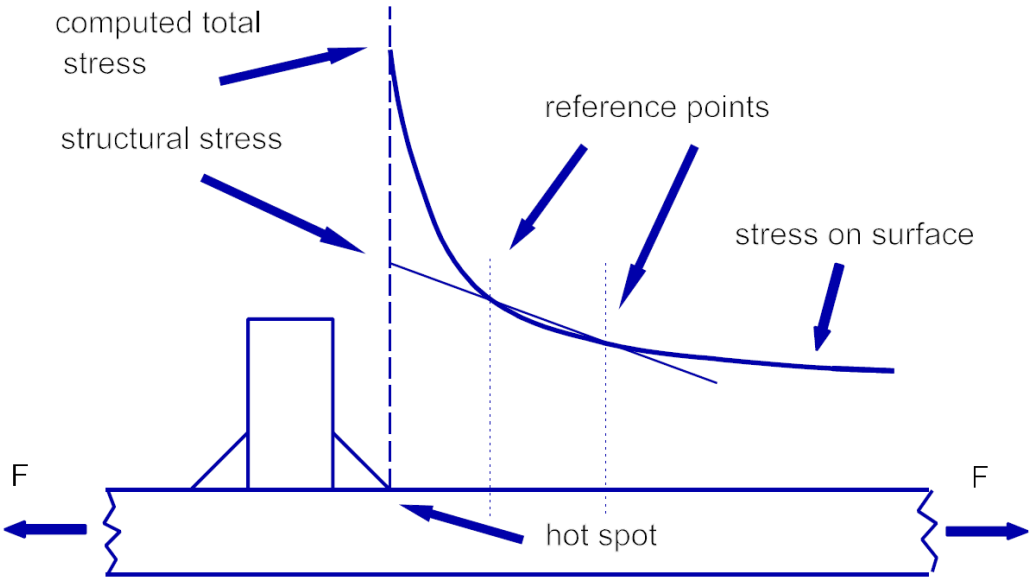

Figure 3. Hot Spot stress definition. (Hobbacher 2014)

Hot spot is divided as two types a and b depending of the location on the plate and orientation to the weld toe. These two types are shown in figure 4.

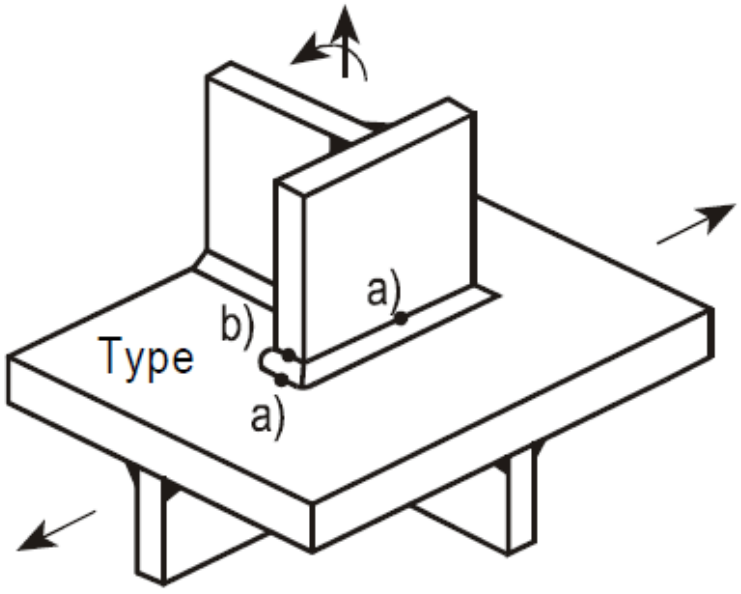

Figure 4. Hot spot types. (Hobbacher 2014)

Hot spot calculation depends on type and in this case, it is type a. Calculation of structural hot spot stress depends on also mesh quality and there are different approaches for fine and coarse mesh as following equations presents. (Hobbacher 2014)

$$\sigma_{hs} = 1.67 * \sigma_{0.4*t} - 0.67 * \sigma_{1.0*t} \quad (8)$$

$$\sigma_{hs} = 1.5 * \sigma_{0.5*t} - 0.5 * \sigma_{1.5*t} \quad (9)$$

$$\sigma_{hs} = 2.52 * \sigma_{0.4*t} - 2.24 * \sigma_{0.9*t} + 0.72 * \sigma_{1.4*t} \quad (10)$$

In equation (8), (9) and (10) *t* is plate thickness. Equation (8) is being used with fine mesh when element length is no more than 0.4 * *t*. When the mesh is more coarse equation (9) is being used. Equation (10) is being recommended to use with thick-walled structures, pronounced increasing non-linear structural stress towards the hot spot area or direction of the applied force changes sharply. In type b hot spot stress distribution isn't dependent on plate thickness thus reference points are at absolute distances from the weld toe or end of the weld. In this case following equations can be used. (Hobbacher 2014)

$$\sigma_{hs} = 3 * \sigma_{4\ mm} - 3 * \sigma_{8\ mm} + \sigma_{12\ mm} \quad (11)$$

$$\sigma_{hs} = 1.5 * \sigma_{5\ mm} - 0.5 * \sigma_{15\ mm} \quad (12)$$

Equation (11) can be used with fine mesh when element length is no more than 4 mm at the hot spot area and equation (12) is for coarse mesh where element length is 10 mm at the hot spot area. (Hobbacher 2014)

2.2.2 4R-method

4R-method is a fatigue life estimation which is based on effective notch stress (ENS), the Smith-Watson-Topper (SWT) mean stress correction and local strain methods which takes account residual stresses σ_{res}, material strength R_m, weld toe radius *r* and applied stress ratio *R*. Unlike conventional methods such as ENS or Hot Spot which use traditional strain-life

curves 4R-method results continuous master curve which is based on fatigue tests from the literature and fatigue tests made by Laboratory of Steel Structures at LUT.

Defining local stress ratio R_{local} is used SWT approach and Neuber's rule. For material properties are used Ramberg-Osgood relationship. 4R- basic equation based is based on as follows (Nykänen, Björk. 2015. p. 582):

$$N_f = \frac{C_{ref}}{\left(\frac{\Delta\sigma_k}{\sqrt{1 - R_{local}}}\right)^{m_{ref}}} \tag{13}$$

In equation (13) N_f is calculated lifetime, C_{ref} is fatigue capacity, $\Delta\sigma_k$ is effective notch stress and m_{ref} is slope of reference curve. When the data is obtained from the test specimens curve fitting is done by minimizing of the sum of squared perpendicular distances, on the other hand, using the Demig regression (MSSPD-approach). This results continuous S-N curve. Process flow can be seen in figure 5.

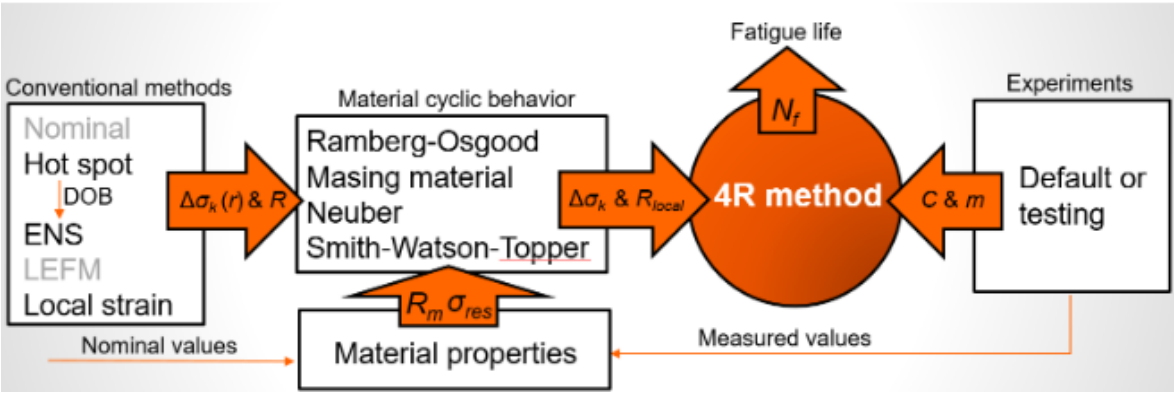

Figure 5. Master S-N curve in 4R-method. (Ahola 2018).

4R-method as a tool requires from test specimen residual stress, material ultimate strength, stress ratio as result from loading and stress amplitude from FE-model analyzed by ENS-method. ENS-method takes account weld toe radius when calculating notch stress. With these parameters is calculated maximum and minimum stress values by using material cyclic behavior. These values are used to calculate R_{local} and with this fatigue lifetime can be obtained.

3 MEASUREMENT AND FATIGUE TEST PROCESS

This part consists of designing strain gauge measurements for the trailer's frame and the designing of fatigue test to the most critical weld. Measurement designing incudes FE-modeling to both frame measurements and fatigue test specimen. Based on the strain gauge measurement results fatigue life analyzes are made.

3.1 Defining of loads

Trailer's frame is exposed to static and fatigue loads as it is being used empty and with cargo. In the measurements was used trailer with the most carrying capacity and thus it gives maximum static and dynamic loads and fatigue loads.

Static loadings are from structure's own weight and cargo. Trailer's own weight is 7.8 t and maximum load capacity is 35 t which is 343 kN. Cargo's weight was measured from truck's air suspension system and checked with factory's weighing scale. The most dominating values from static loading are shear force at bearing and vertical bending moment between front and back axels.

Trailer is exposed to various fatigue loadings during work cycles and thus in strain gauge measurements was continuous long period. This period included usage at three different road types with and without cargo, loading and unloading to measure real life usage. From this measurement is done rainflow analysis which can be used to define equivalent loadings. Fatigue loadings results from irregularities in road, turns and vibrations of timber bunks when driving without cargo at high speed. Due to frame's ladder structure deformations at turns with cargo are significant. The front of the frame is more rigid because of the bearing structure and rear part of the frame is more flexible.

3.2 Measurements of trailer's frame

Measurements were designed to define certain loads to the frame. The measuring points were selected in close cooperation with client's experience of most critical points and with our experience.

3.2.1 Goal and purpose of the measurements

The goal of the measurements is to determine global maximum forces and the most critical point's affecting forces. These loadings are used to improve already existing product and furthermore for new designs. Measurement data is used to verify FE-model results and to calculate fatigue lifetime for the most critical welded detail.

3.2.2 Measurement plan and targets

Measurement points were roughly decided at the first meeting and after that FE-model was made to determine exact points to be measured. From FE-model was analyzed two different loading types. First was with cargo load to define bending moment distribution and thus maximum global bending moment in vertical direction. This distribution can be seen in figure 6.

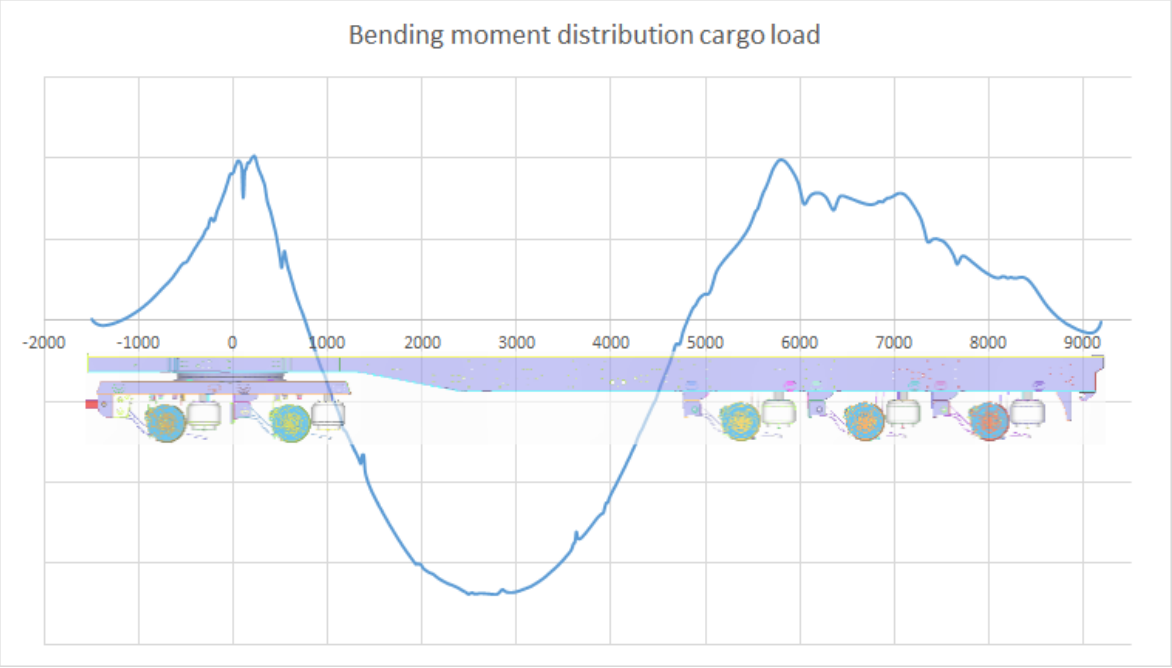

Figure 6. Global bending moment distribution in vertical direction.

In figure 7 is shown horizontal bending moment distribution when front tandem axels are pulled in 90-degree angle, directly sideways, in reference to frame.

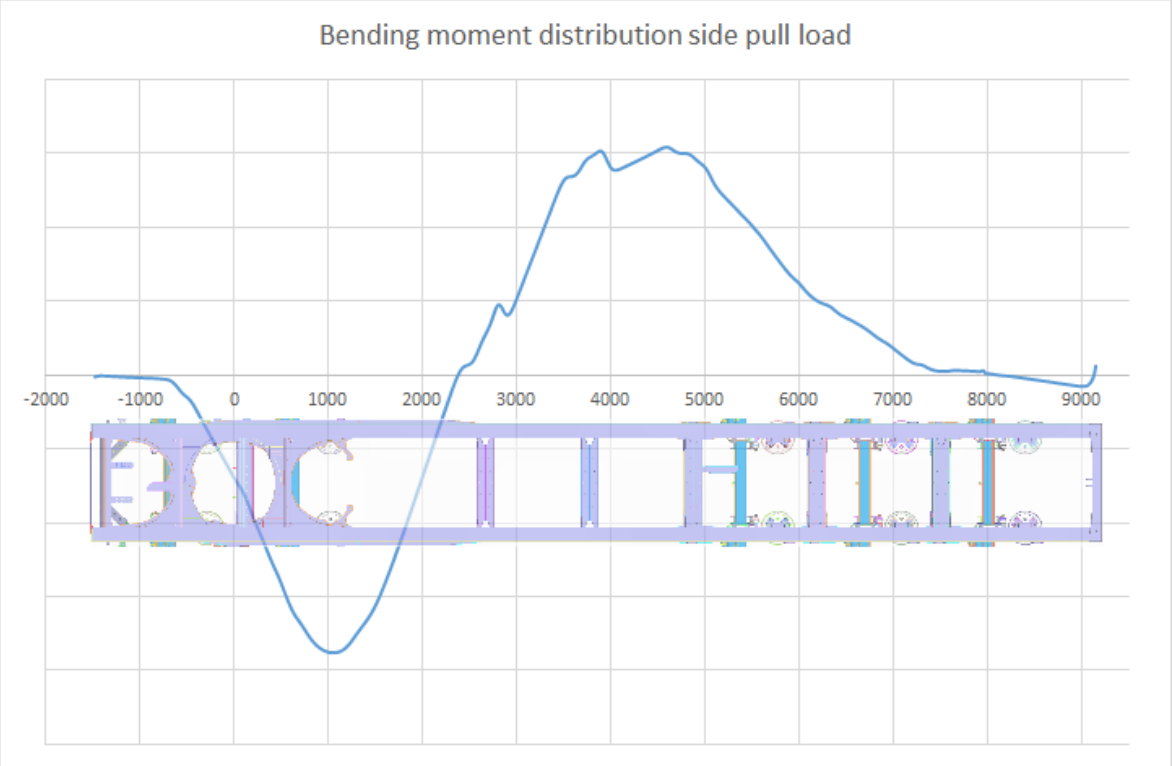

Figure 7. Global bending moment distribution in horizontal direction.

In both figures 7 and 8 distributions are in length direction and zero point is at the center of bearing. Bending moment distributions were obtained by listing node's stresses in length direction from flange and web and multiplied with moment of inertia in relation to corresponding direction. These two bending moment distributions combined were used to establish the most effective place in the frame to measure both global bending moments with same strain gauges. Due to moving timber bunks only three strain gauges were put in place per longitudinal beam. This mean that simplification based on the symmetrical structure was needed.

By established conversations with client and FE-models measurement plan consists total of 13 strain gauges and two acceleration sensors. Two gauges are placed at hot spot distance to third axel's bracket's weld (SG 1A & 1B). Two gauges are measuring shear force at beam's web plate near to the bearing (SG 2A &2B). Six gauges are placed between first and second of five transverse beams at I-beam's flanges (SG 3 LA-LC & RA-RC). These measures horizontal and vertical global bending moments in length direction. One strain gauge is at first transverse beam's bracket to measure compression and tension (SG 4). Last two gauges are at I-beam's necking point where one gauge is placed on the bottom side of the flange and

the other one is at the web plate (SG 5A & 5B). Both measures normal force in length direction. Two acceleration sensors are placed on both ends diagonally to measure structural dynamical behavior and to help analyzing the data (ACC_E & ACC_T). Strain gauges and accelerations sensors positions are shown in the figure 8.

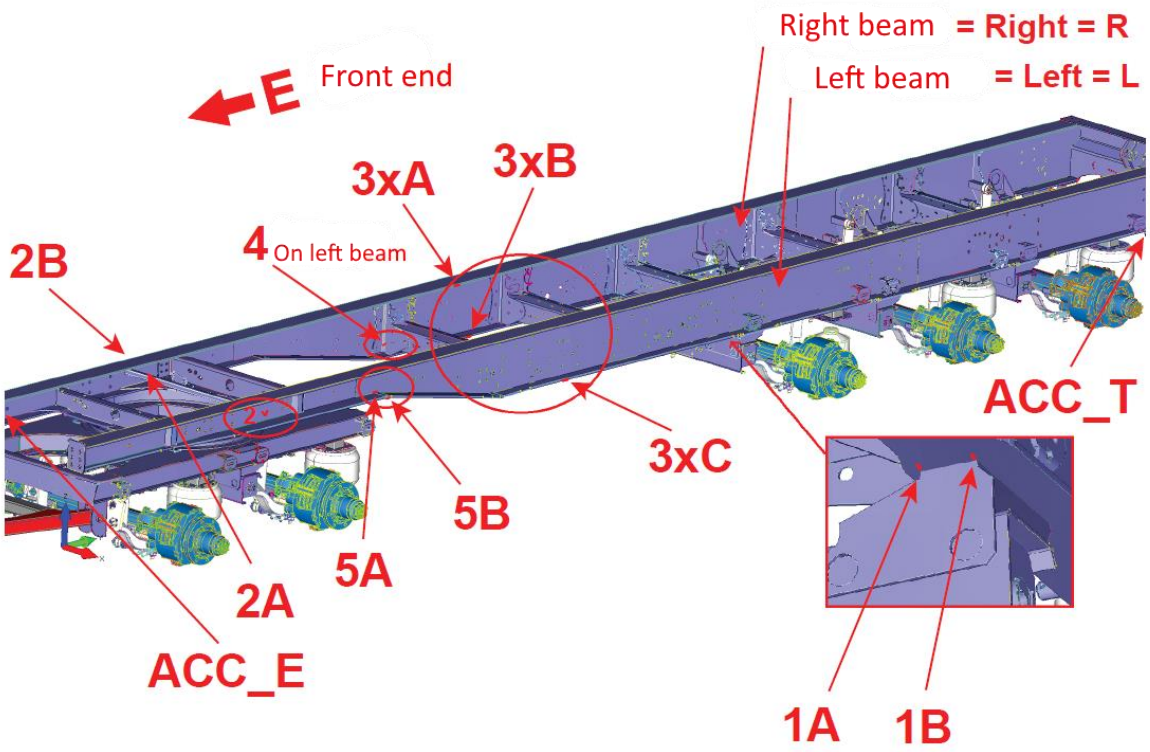

Figure 8. Strain gauges positions.

Due to the trailer's accessory installations strain gauges 3&4 couldn't be installed on the same side as the other gauges but structure is symmetrical and thus gives reliable information. Strain gauges' and acceleration sensors' detailed information is presented in following table 1.

Table 1. Measuring equipment's information.

Measuring point	Strain gauge type	Configuration	Measured value	Observation	Quantity
SG 1A&B	Single gauge	1/4	Normal force	Hot Spot distance	2
SG 2A&B	V-gauge	1/2	Shear force		2
SG 3 LA-LC & RA-RC	Single gauge	1/4	Bending moment		6
SG 4	Single gauge	1/4	Normal force		1
SG 5A&B	Single gauge	1/4	Normal force		2
ACC E&T					2

Strain gauge pictures were taken and are credited by Vesa Järvinen from Unisigma Oy. In figures 9 and 10 is presented examples of strain gauge positions from in front of third axel where hot-spot stress was measured from both weld's corners.

Figure 9. Strain gauges 1A and 1B.

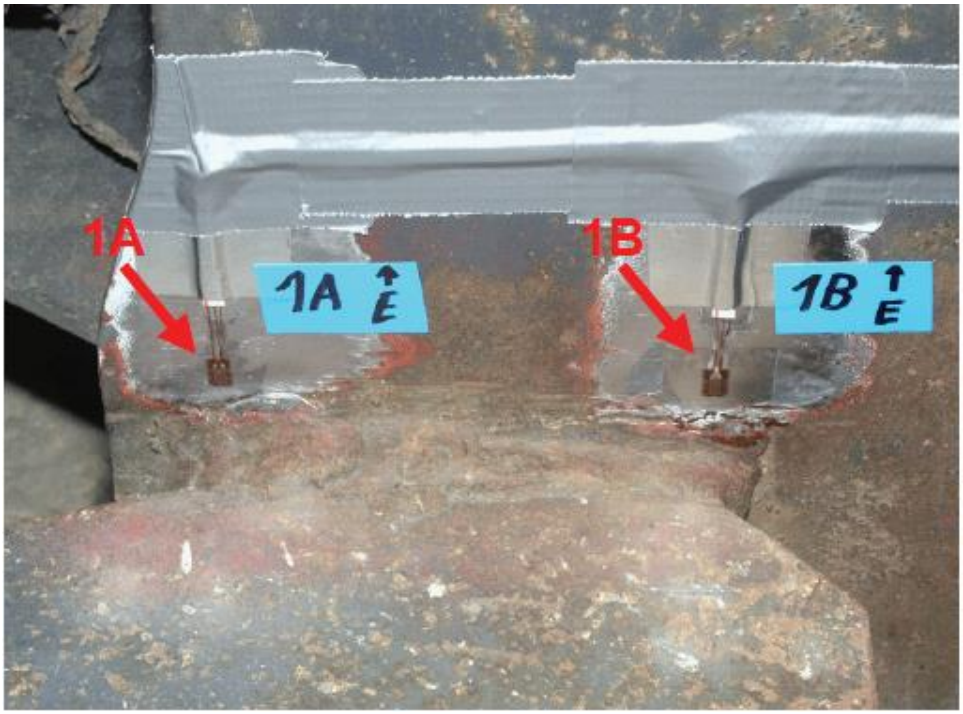

Figure 10. Strain gauges 1A and 1B positions.

In figure 11 is shown strain gauges 3LA and 3 LB which are measuring longitude stresses for global bending moment. Gauges were placed to the sides of flanges due to timber bunk's movement.

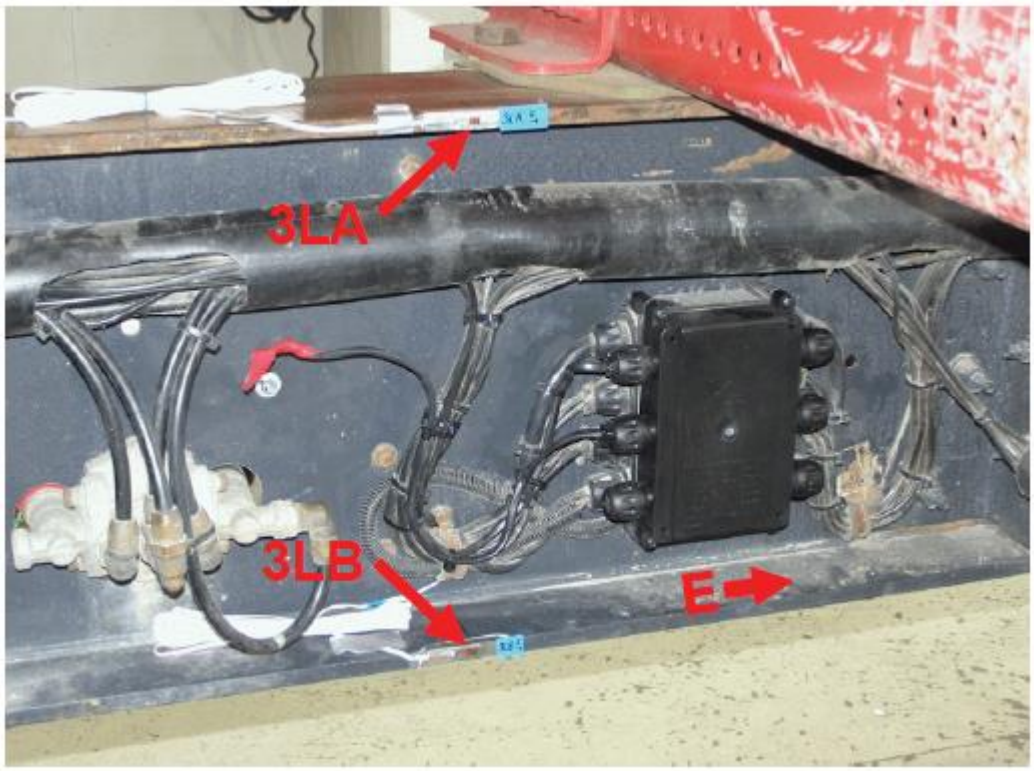

Figure 11. Strain gauges 3LA and 3LB positions.

The rest of the strain gauges placement and installation is presented in appendix II.

3.2.3 Execution of measurements

Measurements were made at Jyki Oy besides continuous measurements which were done at Längelmäki area as part of normal cargo deliveries. Installation of measurement equipment, strain gauge and acceleration sensors were made by Vesa Järvinen from Unisigma Oy. He was also the participant party at continuous measurements and observed the single event measurements.

The first measurement was continuous measurement because the truck wasn't available at first and the timetable was more suitable for that. Continuous measurement that lasted two days was done 23-24.7.2018. As in measurement plan can see (Appendix I) 4.1-6 consists of driving on three different types of roads with and without cargo. Used cargo was full load

of 5 m long timber and thus two piles. The measurement was done for 24 h and in two 12 h shifts. This was less than originally designed but gave still enough reliable and variable data. Next measurements were single events and static measurement which were conducted 25.7.2018 at Jyki. In static measurement trailer was loaded with two 5 m long log piles. This measurement gave the reference point to other measurements and informed the magnitude of forces at stationary position. After static reference measurement was all single events with full cargo. First were events 3.1- 3.5 where trailer was driven over two different transversal obstacles with both tires and other side's tires. 3.1- 3.4 situations represented driving over a curb with different speeds. Obstacle was made of 75 mm high wood beam that was supported with gravel. 3.5 event was made to air suspension reach maximum clearance and used obstacle was 90 mm high gravel bump. 3.6 event was 90 degree turn over building corner with higher speed and full cargo. This gave measuring data from extreme conditions of driving. 3.7 and 3.10 events were conducted to get side pull load measuring data with and without cargo. In these events the trailer was reversed to position where front tandem axels were in 90-degree angle in relation to frame. Event started in stationary position and trailer was pulled straight. In events 3.8 and 3.9 truck was driven in 8-shape and turns were made as tight as possible. 3.8 situation doesn't represent actual real condition unless mechanism is broken because automatic system prevents last axel to rise if load is too much. Event 3.11- 3.14 were the same as 3.1- 3.5 but trailer was driven empty.

3.2.4 Processing measurements' results

Raw measurement data was sets of points which were taken from strain gauges with 1 ms increments. The time increment defines how accurate the results are thus smaller increment means more accurate results. This data was processed with InField program which converted these point sets to strain-time charts. Charts were divided to different measurement cases by base time which was running time from the beginning of the measurements and measurement logs. The data was filtered with low-pass filter

Single measurement events were used to define structure's static and dynamic stresses and forces. Static and two dynamic results were compared to FE-models' for verification purposes. Other dynamic events' results were used to obtain dynamic magnification factors. These factors reflect the structure's behavior under dynamic loadings and how these loading affect to the structure. Single events' results were also used to compare to the continuous

measurement to find out how accurately those events reflects real life situations. In figure 12 is an example of static and dynamic strain relation in single event.

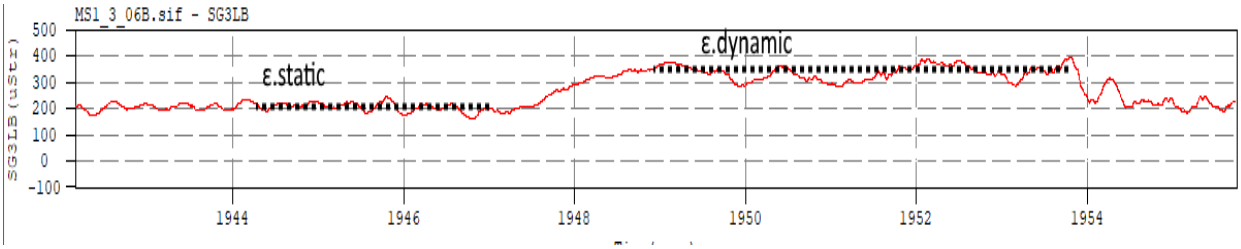

Figure 12. Static and dynamic strain relation in single event.

Continuous measurement data was divided by road type and was it driven with or without cargo. From all these different sets were done rainflow analyses to define affecting stresses at third axel's bracket. Rainflow analyses were obtained from raw data in 2D formation which represents quantity of cycles with different combinations of mean stresses and stress ranges. Rainflow analysis was used to determine bracket's weld lifetime by 4R-method.

3.3 FE-analysis

In FE-analysis was used Femap software and Nx Nastran solver by using linear static analysis. FE-model was created from whole trailer's frame to define final strain gauge positions and to understand how the structure behaves under loading. Two different models were used for two load types. One was for full cargo loading at stationary position and the other one for side pull loading without cargo. These models' results gave the maximum global loadings and local stress points.

3.3.1 FE-model and execution

Models were mainly made by using mid-surfaces and meshing those with plate elements. A few details were made by using solids which were meshed with hexagonal solid elements. Rivet connections were made by rigid and beam elements. Chassis were simplified by using beam and spring elements because those were standard parts and thus weren't the focusing point. Connections were made as frictionless connections and tires were modelled with springs. In static position dampers won't have effect to the structure thus those were left out of the models. Air suspension was modelled with spring elements which had individual compression stiffness in each axel in relation to amount of vertical loading. In both loading

cases linear static analysis was being used. In figure 13 can be seen all the plate thicknesses and model's structure.

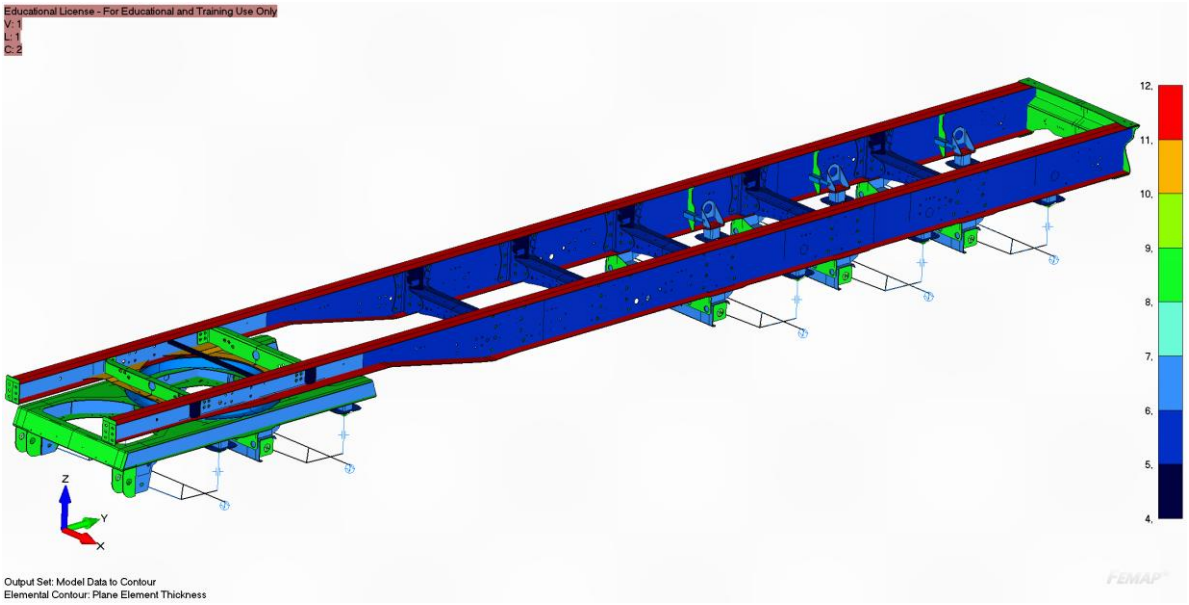

Figure 13. Fe-model's plate thicknesses.

Two separate FE-models were made to two different load cases: cargo load and side pull load. In both cases own mass is not taken account as the strain gauges are calibrated to be zero with it. Cargo load is evenly distributed area force 343 kN to the top flanges and to side pull load is estimated 3 kN from the front sub frame to the side in 90° angle. Estimation is based on calculation where the whole cargo mass will just start moving. These load cases can be seen in figures 14 and 15.

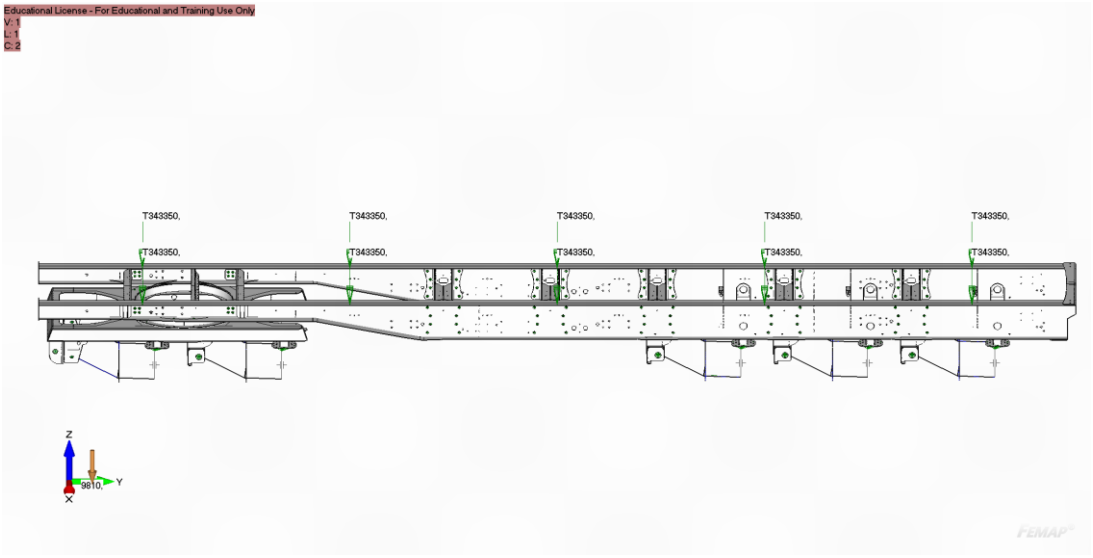

Figure 14. Full cargo load.

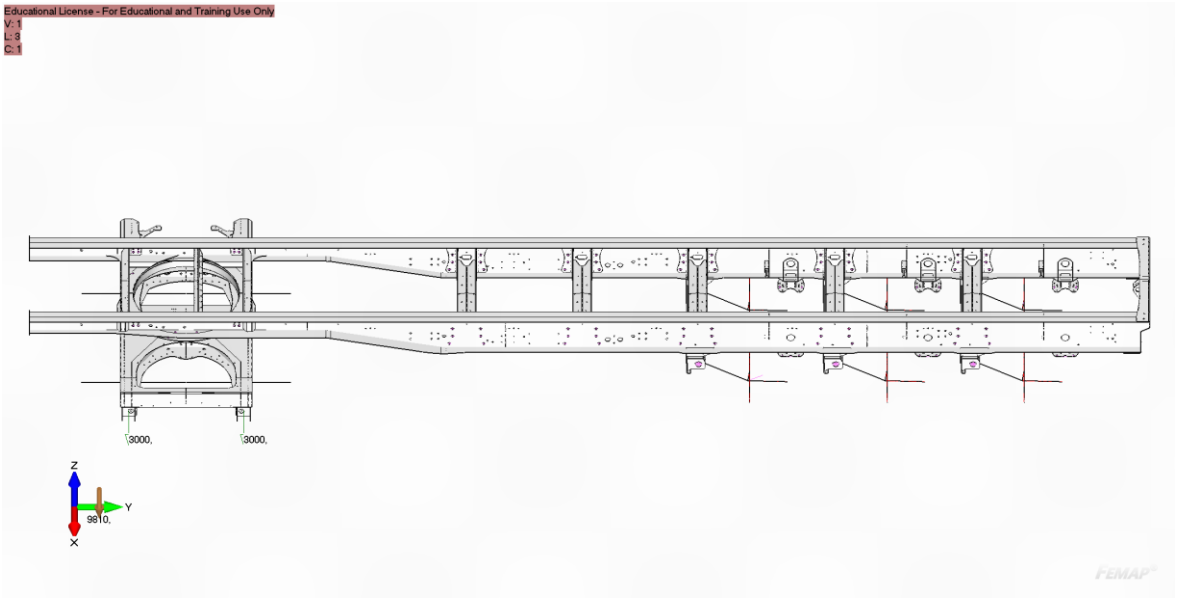

Figure 15. Side pull load.

Trailer's structure was mainly made of Strenx 650 MC steel in exception of the I-beams' flanges which were made of Strenx 700 MC + steel. Materials' properties can be seen in the table 2.

Table 2. Material information. (SSAB 2018a & SSAB 2018b)

Material	Thickness [mm]	Yield strength [MPa]	Tensile strength [MPa]	Young's modulus [MPa]
650 MC	3.01–6.00	650	700–850	210 000
700 MC +	10.01–12.00	700	750–950	210 000

3.3.2 Verification of FE-models' results

Verification was executed by comparing results from strain gauge measurements and FE-models. From strain gauge measurements were selected results that gave the stresses with and without cargo at stationary position and event 3.10 which was side pull from 90° angle without cargo. These results were compared to the FE-models' stresses at strain gauge positions.

3.4 Execution of 4R-method

The base for 4R-method was 2D-rainflow analyses of strain gauges that measured structural hotspot stress at 0.4 * *t* distance from weld toe. These alone weren't enough to measure hotspot stress thus stresses at 1.0 * *t* distance were obtained from FE-model. Because hotspot stresses cannot be directly be used for 4R-calculation, those are needed to be converted to ENS stresses. Hotspot and ENS stress have relation as can be seen from following equations (Ahola et al. 2016. p. 670-682):

$$\sigma_{hs} = \sigma_m + \sigma_b \tag{14}$$

$$\sigma_k(r) = K_{t,m}(r) * \sigma_m + K_{t,b}(r) * \sigma_b \tag{15}$$

In equation (15) $K_{t,m}$ is membrane stress factor and $K_{t,b}$ is bending stress factor. These factors weren't possible to obtain from FE-models due to variation in values which was caused by different types of loadings. Thus, ENS and hot spot stresses were compared directly, and correlative factor was found. In ENS-model only inspected weld was modelled with fine linear solid mesh. ENS-model can be seen in figure 16.

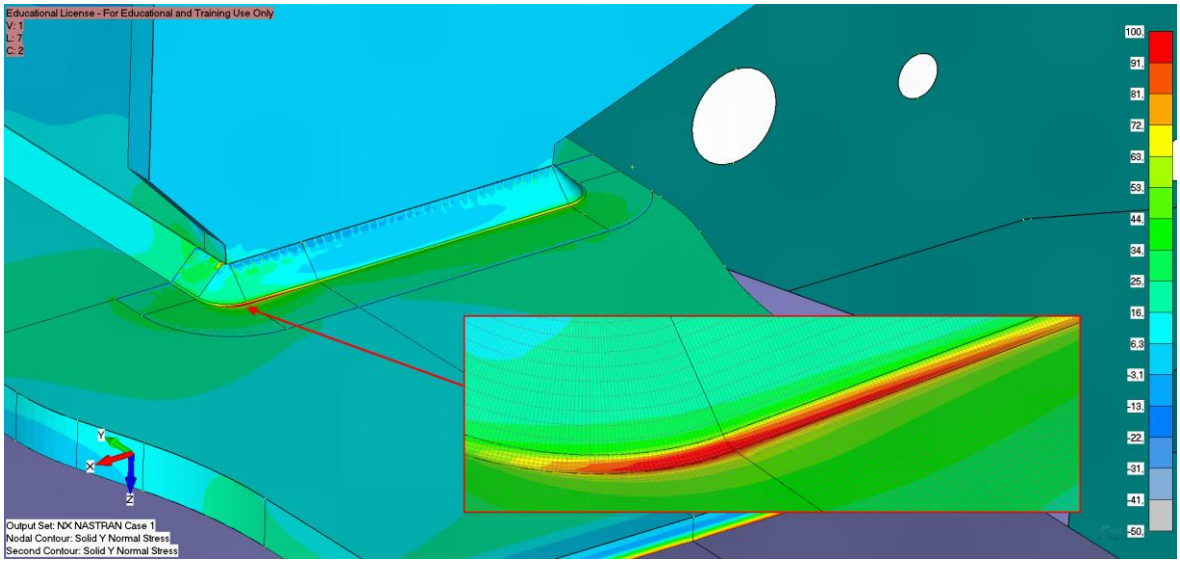

Figure 16. ENS model.

The weld's 3D geometry was scanned to define true weld toe radius for ENS model. The measuring area and 3D-scanned area can be seen from figure 17 and 18.

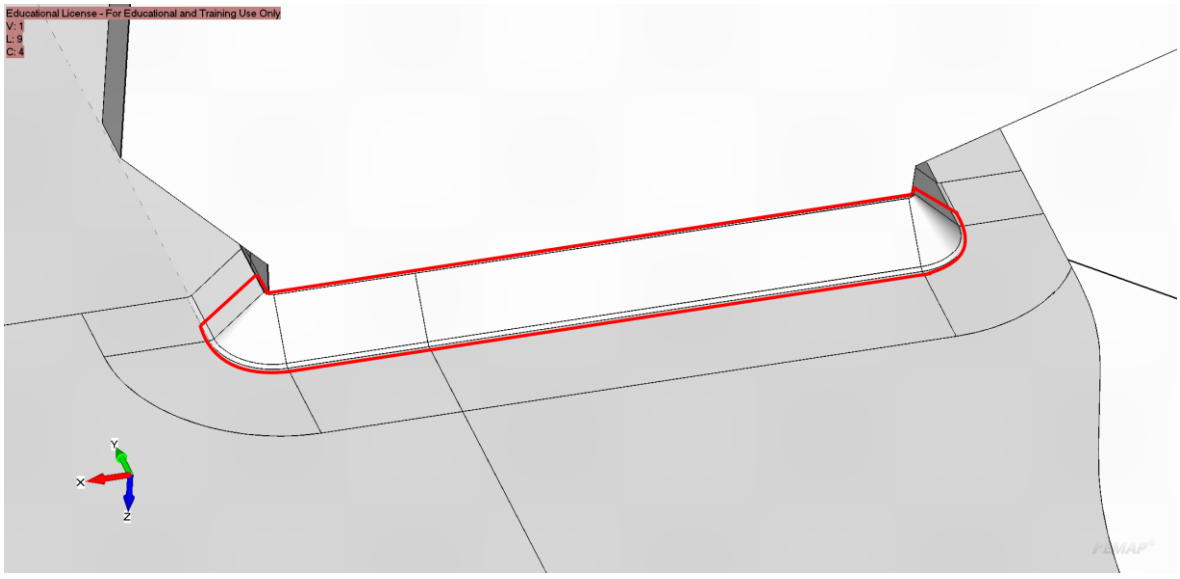

Figure 17. Measuring area of weld's true 3D geometry.

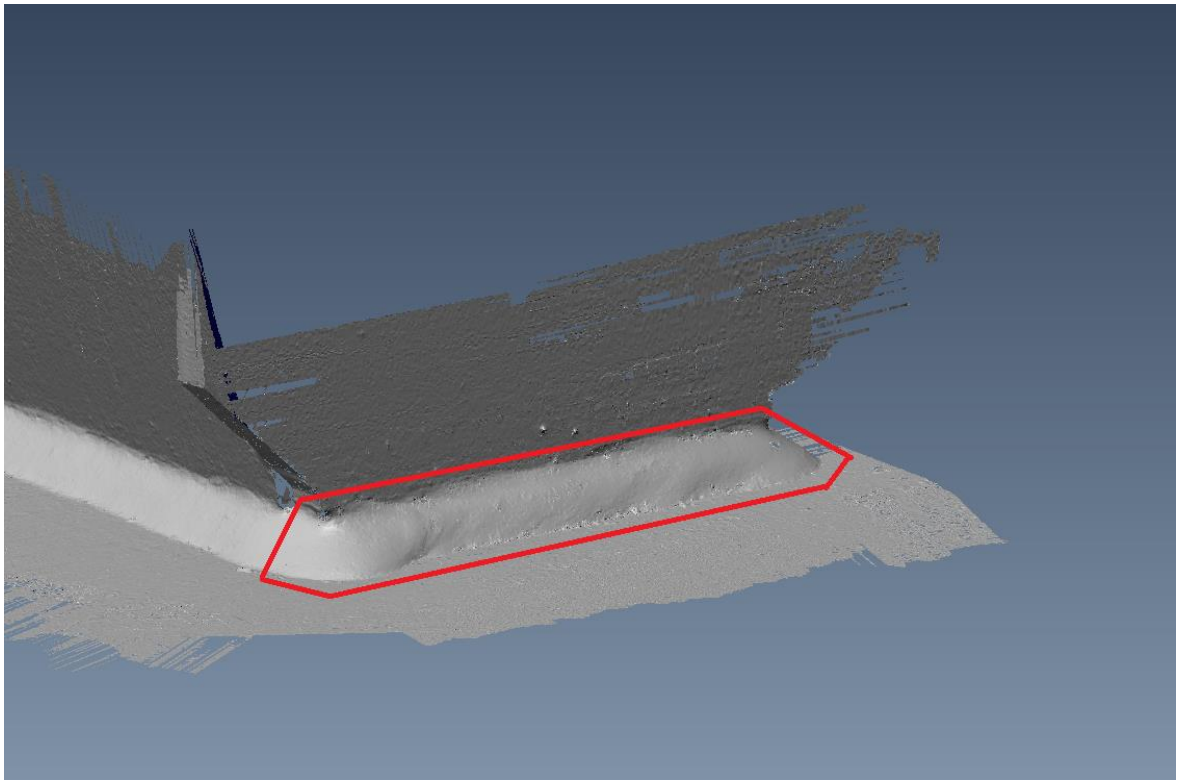

Figure 18.

From the 3D-scanned weld geometry the true weld toe radiuses were measured. Weld toe radius was measured from both weld corners where the strain gauges were located. The smallest weld toe radius from this area was also located and measured as it drives the failure. From the corners weld toe radiuses were 1.8 mm and 0.88 mm and can be seen in figures 19 and 20.

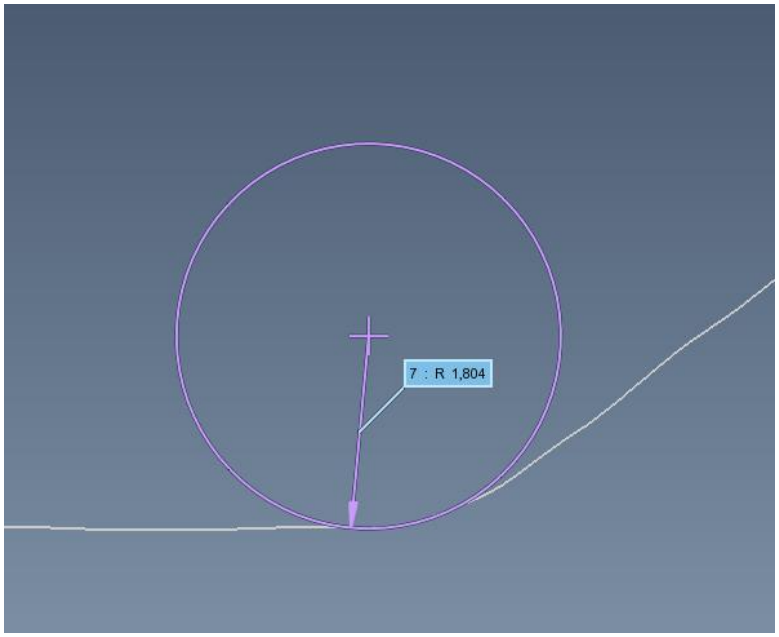

Figure 19. Weld toe radius at the corner of the weld.

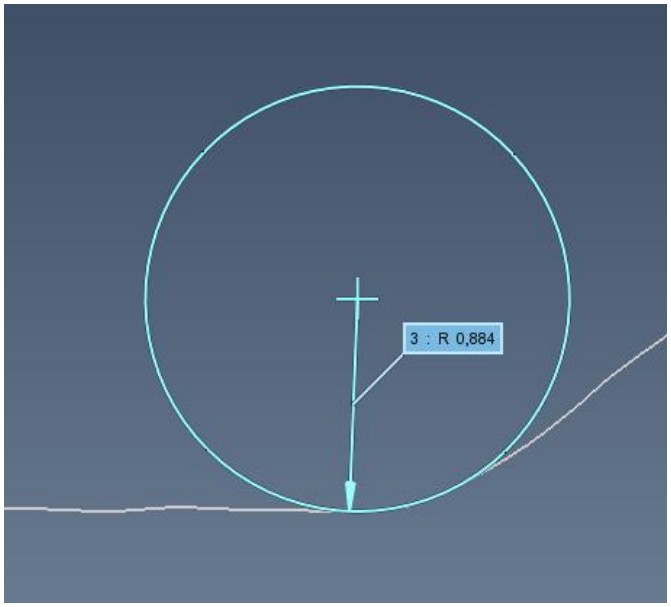

Figure 20. Weld toe radius at the corner of the weld.

The smallest radius was 0.12 mm which seemed to be the end point of weld. In ENS-model was used the most critical radius 0.12 mm + 1 mm. This radius measurement can be seen from figure 21.

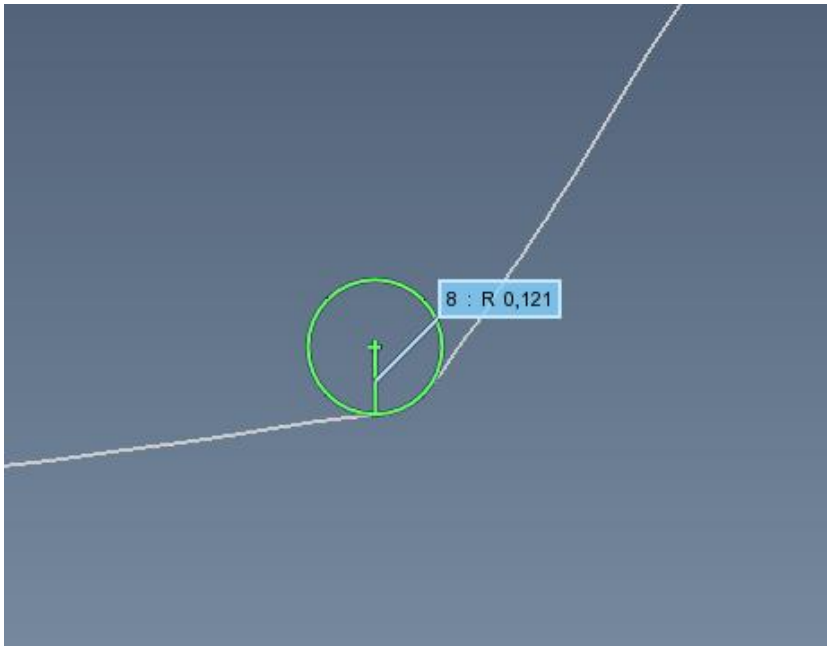

Figure 21. The smallest weld toe radius of the weld.

Weld's residual stresses were measured from both corners at the weld toe, hot spot distance 4.8 mm and 15 mm distance from weld toe. The strain gauges were positioned to these hot spot points. Measuring points are presented in figure 22 and measuring equipment and event can be seen in figure 23.

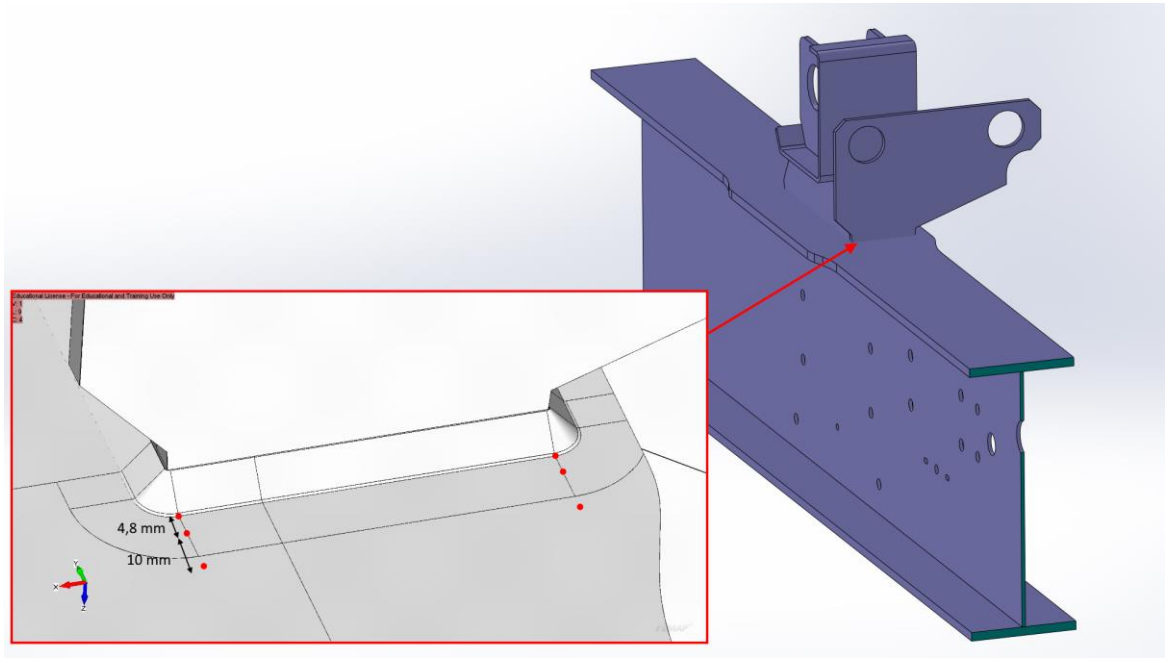

Figure 22. Measuring points of residual stresses.

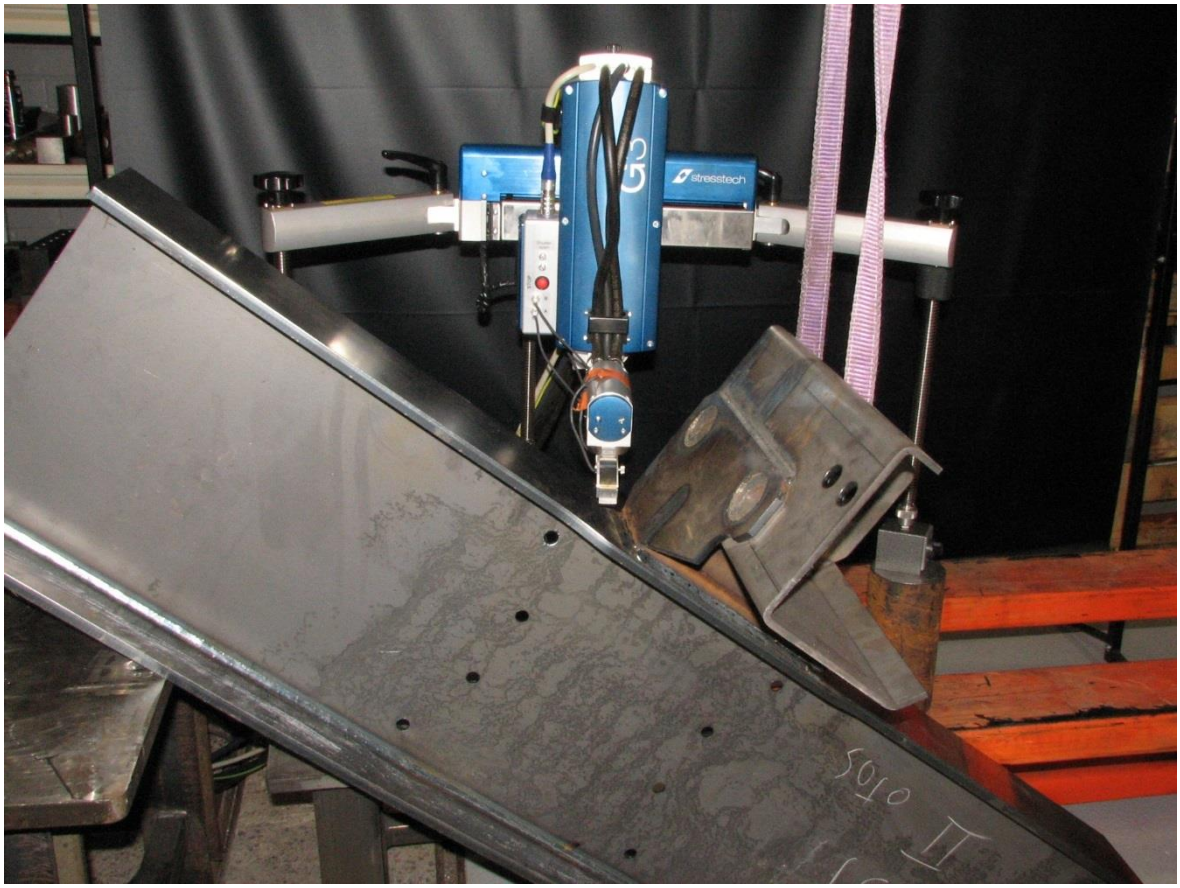

Figure 23. Residual stresses' measuring equipment and event.

3.5 FAT-class test

Based on the FE-models' and strain gauge measurements the most critical point of structure was selected to be the third axel's bracket's weld. This weld's lifetime was calculated by 4R-method thus its true FAT-class was wanted to be tested. The test was four-point bending test where both end supports were able move in longitude direction. The the beam was loaded with intermediate beam and hydraulic jack trough high strength steel ball to minimize bending stress in the cylinder piston. The test setup can be seen in figure 24.

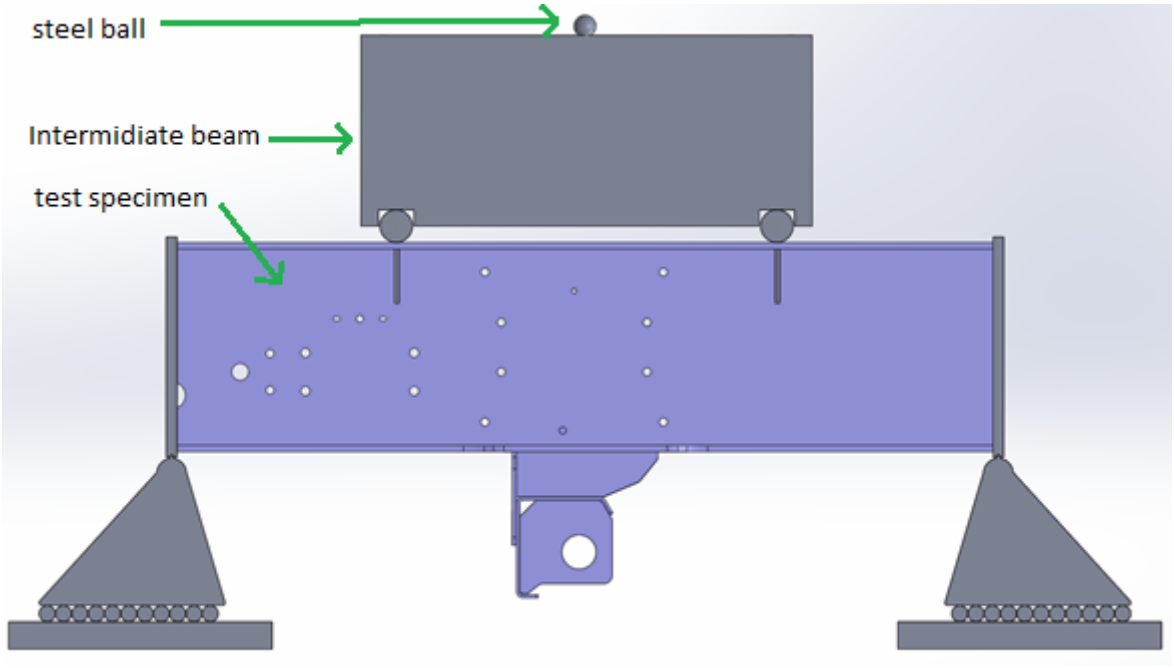

Figure 24. Test setup.

FE- model was created from the test specimen first to configurate the distance between the pressing lines to get only bending stress to the observed weld area. The second tested value was pressing force as the stresses at the weld toe needed to be high enough to last approximately 100 000 cycles by ENS-calculation. In FE-model the constraints were assigned to both ends of the beam. For one end all translations were supported and for the other end x- and z-direction were supported. This allowed the translation in the longitude direction and free rotation. The loading was assigned as forced translation to get even translations/forces through width of the flange. This resulted some iteration for the forced translation as the pressing force was read from the analyze output's constraint forces. FE-model's loadings and constraints can be seen in figure 25 and bending stresses in figures 26 and 27.

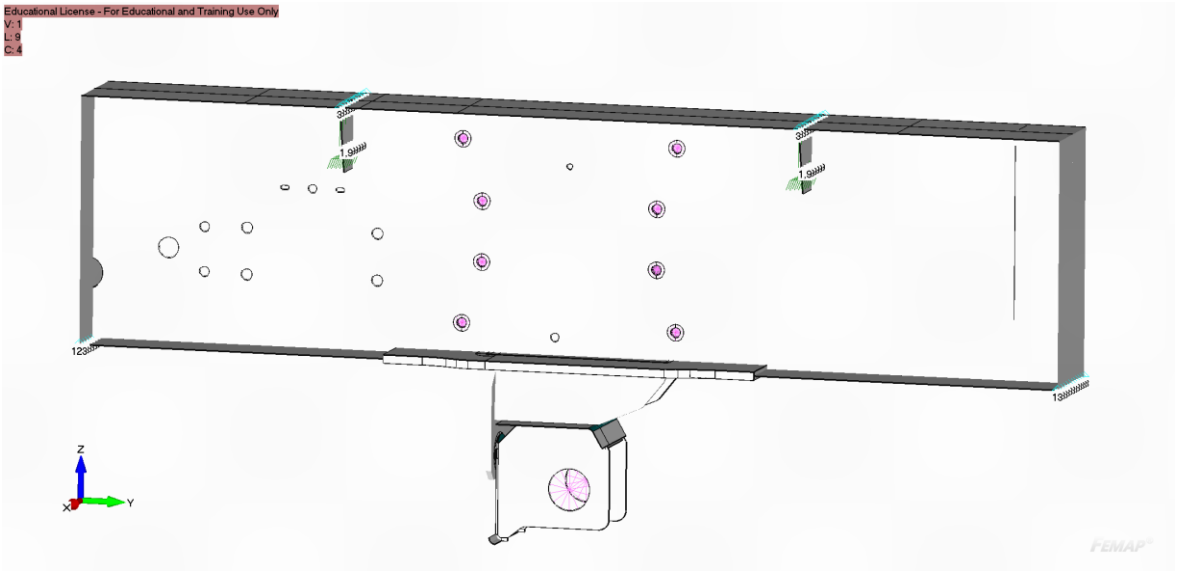

Figure 25. Fe-model of the test specimen.

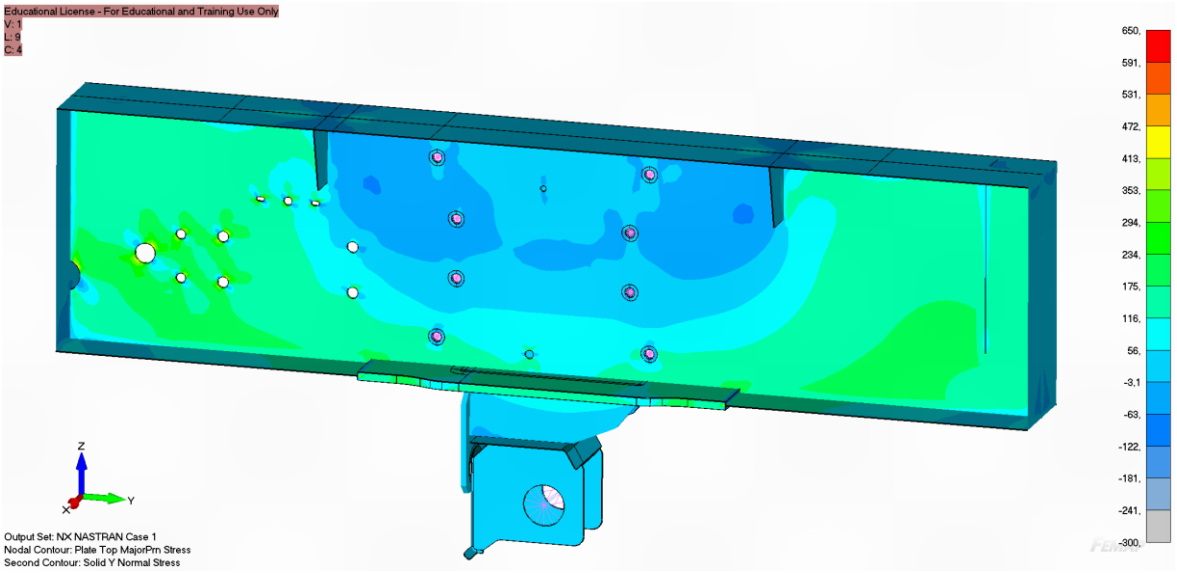

Figure 26. Test specimen's bending stresses.

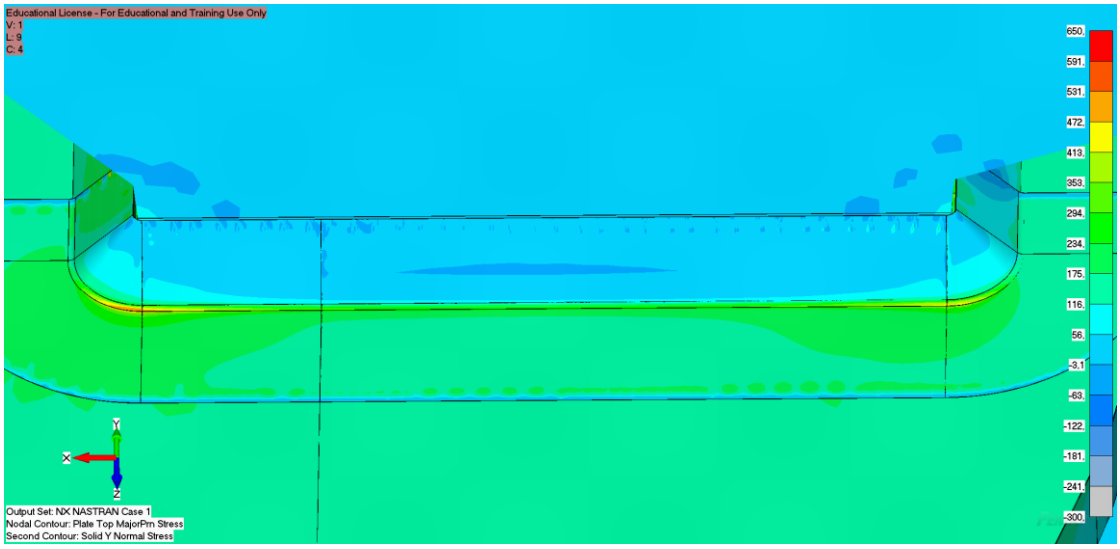

Figure 27. Stresses at the weld of the test specimen.

FE-analyzes were conducted for intermediate beam as it was designed to last for multiple tests in the future. This was only done to check that there won't be excessive stresses in the pressing tool or pressing bars. For that purpose, the tool was made from solid steel that had milled holes for the bars and drilled controlling hole to the ball between pressing tool and cylinder's head's tool. The stresses and FE-model of the pressing tool can be seen in figure 28.

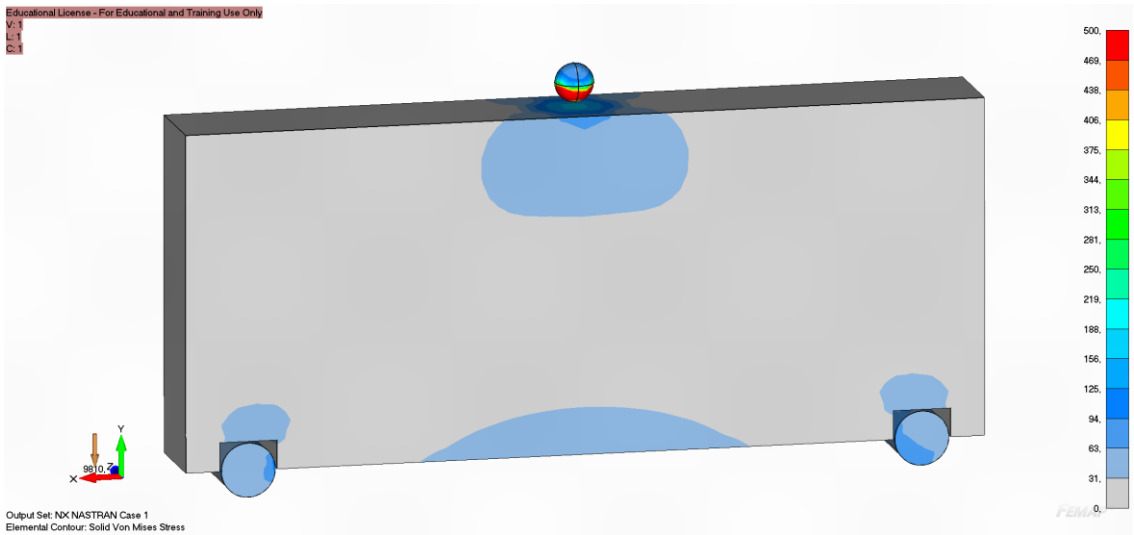

Figure 28. Test setup.

High stresses at ball surface are partly caused by the contact in FE-model as it was simplified, and the beam's contact surface was flat.

4 RESULTS

The results part consists of results from strain gauge measurements, FE-models, 4R-method's calculations and FAT-class test. These reflects the static and fatigue strength of the trailer's frame.

4.1 Results of strain gauge measurements

The first goal of strain gauge measurements was to define static stresses with cargo load and empty trailer and compare those to FE-models' stresses and analyze how much difference is there. These static results were taken before unloading and after empty trailer had time to stabilize due to brakes being applied at stationary position. Still the ground roughness could have been affecting to the results. In strain gauge measurements the cargo load was 34 t and in FE-model it was 35 t. Those results can be seen in table 3.

Table 3. Stresses at stationary position.

	Measurement		Fe-model	
	Cargo [MPa]	Empty [MPa]	Cargo [MPa]	Empty [Mpa]
SG1A	117	37,1	49	1,6
SG1B	47	10,5	64	2
SG2A	-12	-3,3	-58	-1,4
SG2B	-14	-1,5	-44	-1,1
SG3LA	-20	2,2	-57	-1,7
SG3LB	44	6,7	56	1,6
SG3LC	28	-2,7	68	2,2
SG3RA	-67	-11,7	-58	-1,7
SG3RB	11	-4,7	54	1,5
SG3RC	48	4,3	67	2,1
SG4	41	-1,9	37	-1
SG5A	32	-5,1	65	3,1
SG5B	93	7,0	84	1,8

From these results can be seen that FE-models' results distinguish from the strain gauge measurements as FE- model's results are more on the same level. The most noticeable stress difference is in SG 1A and 1B. All of those have multiple times higher stress levels with cargo. This static strain gauge measurement results for SG 2 shear force and SG3s vertical bending moment according to table 4.

Table 4. SG 2 shear force and SG3s bending moments.

	Measurement	Fe-model
Vertical bending moment [kNm]	30	47
Transverse bending moment [kNm]	8,4	19
Shear force [kN]	65	255

Transverse bending moment in table 4 is taken from single events 3.7 where trailer was pulled from 90-degree angle. Single events' strain gauge stresses peak values were divided by static stress values and thereby absolute dynamic stress multipliers were calculated. These multipliers can be seen in table 5.

Table 5. Dynamic multipliers from single events.

	Dynamic multipliers													
	With cargo									Empty				
	3.1	3.2	3.3	3.4	3.5	3.6	3.7	3.8	3.9	3.10	3.11	3.12	3.13	3.14
SG 1A	1,1	1,2	1,0	0,9	1,4	1,8	1,4	2,9	2,6	2,5	1,4	1,6	1,4	1,5
SG 1B	2,0	1,9	1,5	1,5	2,2	2,6	1,4	1,9	2,1	3,1	4,6	4,6	4,3	4,7
SG 2A	2,2	3,4	3,3	3,3	3,0	5,8	2,7	2,7	2,0	3,3	6,4	7,3	4,1	7,3
SG 2B	1,8	2,9	2,7	2,7	2,5	4,8	2,7	2,5	1,7	6,5	14,0	14,0	10,2	14,0
SG 3LA	4,1	4,4	3,7	4,0	3,5	5,4	5,4	3,7	1,7	6,2	12,1	13,9	12,8	17,6
SG 3LB	1,8	1,9	1,5	1,7	1,5	1,9	1,4	1,6	0,9	3,0	2,4	3,8	2,5	2,8
SG 3LC	2,8	3,3	2,7	3,0	2,3	4,8	4,3	3,1	0,9	6,1	8,7	10,9	9,6	12,4
SG 3RA	1,3	1,2	1,2	1,1	1,8	2,0	1,0	1,1	0,8	1,2	3,1	3,6	2,8	3,1
SG 3RB	5,1	4,7	5,3	5,0	3,1	7,0	6,8	5,7	4,7	3,5	4,4	4,7	4,4	4,2
SG 3RC	1,7	1,7	1,3	1,4	1,5	2,4	1,0	1,5	0,7	3,9	7,4	8,7	7,6	8,4
SG 4	0,4	0,9	1,0	1,2	1,1	3,3	3,2	4,8	3,1	42,3	17,5	30,8	20,0	24,6
SG 5A	2,5	2,8	2,5	2,6	2,1	2,9	2,7	2,1	1,1	1,8	4,1	5,0	2,6	4,6
SG 5B	1,6	1,7	1,4	1,3	1,5	1,7	1,6	2,0	1,2	9,3	5,7	7,7	4,2	6,6

With cargo the most critical multipliers were from 3.6 and 3.8 events where the truck was driven at 30 km/h speed to a turn at the paved yard and turned slowly at 8-shape with last axel down. On average the dynamic multiplier was 2.5 and the greatest multiplier was from SG 3RB which had the lowest static stresses with respect to others. Without cargo the greatest multipliers are more distributed but most of those are from event 3.12 and 3.14 where trailer was driven over a transverse obstacle with both side wheels and right-side wheels at higher speed. Due to lower static stresses the multipliers are on average 7.7 and the greatest is 42.3 from SG 4 at event 3.10 where trailer was under side pull load from 90° angle.

From these dynamic results the highest average shear force at SG2 gauges was 345 kN, transverse bending moment at SG3 gauges was 91 kN/m and vertical bending moment 88 kN/m.

The rainflow analyses from different road types were used to calculate equivalent stresses to all measuring points. Mainly the highest stresses resulted from forest road with cargo. These stresses and numbers of cycles are presented in tables 6 and 7.

Table 6. Equivalent stresses with cargo.

	Grovel, cargo (MPa)	n	Forest road, cargo (MPa)	n	Paved, cargo (MPa)	n
SG1A	41,4	36362	44,5	19058	25,7	153775
SG1B	21	41626	23,3	21028	14,5	167548
SG2A	7,8	26028	7,4	11980	6,2	75815
SG2B	7,2	23733	6,9	10577	6,1	64899
SG3LA	16,5	21098	18	9013	14,4	52449
SG3LB	8,9	24875	10,5	11984	8,6	67364
SG3LC	10,7	27631	10,7	13292	9,7	88991
SG3RA	19,2	20030	19,7	8758	15,5	54916
SG3RB	8	24308	10,2	11113	8,4	62775
SG3RC	11,3	26452	11,6	11940	10,4	81586
SG4	19,6	33908	21,3	17144	15	134443
SG5A	11,2	19777	13,7	9026	10	52792
SG5B	15,5	29655	17,8	14046	13	102883

Table 7. Equivalent stresses empty.

	Grovel, empty (MPa)	n	Forest road, empty (MPa)	n	Paved road, empty (MPa)	n
SG1A	22,7	48424	25,7	30502	13,3	160371
SG1B	17,6	46074	22,5	26723	10,7	146050
SG2A	6,8	25581	8,4	17961	4,6	71765
SG2B	5,5	26497	7,2	17876	4	71535
SG3LA	11,8	42945	16,7	26724	8,1	144039
SG3LB	9,6	40042	11,8	26408	6,2	130547
SG3LC	11,2	38081	15,9	23804	7,8	125783
SG3RA	11,5	43398	16,2	27546	8,2	144958
SG3RB	8,9	40036	11	26719	5,8	131645
SG3RC	11,6	37526	16,3	23587	8,1	124756
SG4	16,4	72588	22,7	44994	10,2	231369
SG5A	9,5	28778	12,9	18730	6,5	86797
SG5B	15,4	39519	21	24492	9,9	125540

4.2 Results from fe-analyses

As in the chapter's 3.2.2 was shown the bending moment distribution were calculated from these results. From the cargo loaded FE-model's results can be seen that the bending moment is concentrated between the second and the third axel where is the longest unsupported area.

Due to this concentration the third axel's bracket's connection and behind the bearing where I-beams' web starts to increase have local peak stresses. Elements in the FE-model are aligned to the global coordinate system to match y-direction. Cargo load results can be seen in figure 29.

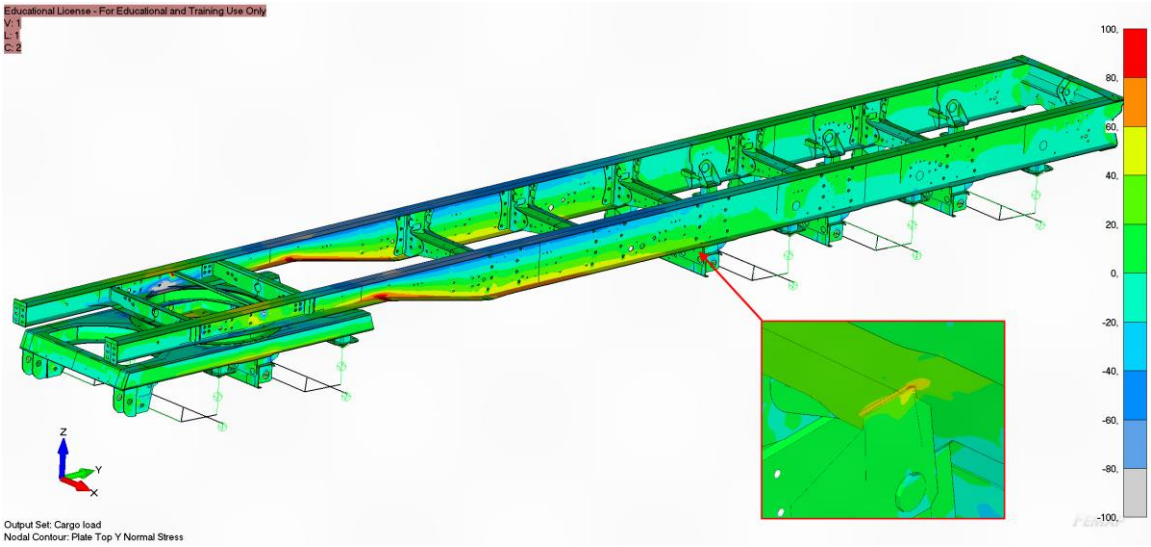

Figure 29. Full cargo load, plate top y normal stress [MPa].

The side load result's stresses and deformation show the behavior of more flexible structure as the transverse U-beams and those connections aren't rigid. Most of the bending stresses are concentrated to area between the front and back axels as in cargo load. Additional stress peak areas are the first three transverse beams' connection plates. These stresses and deformations are shown in figures 30, 31 and 32.

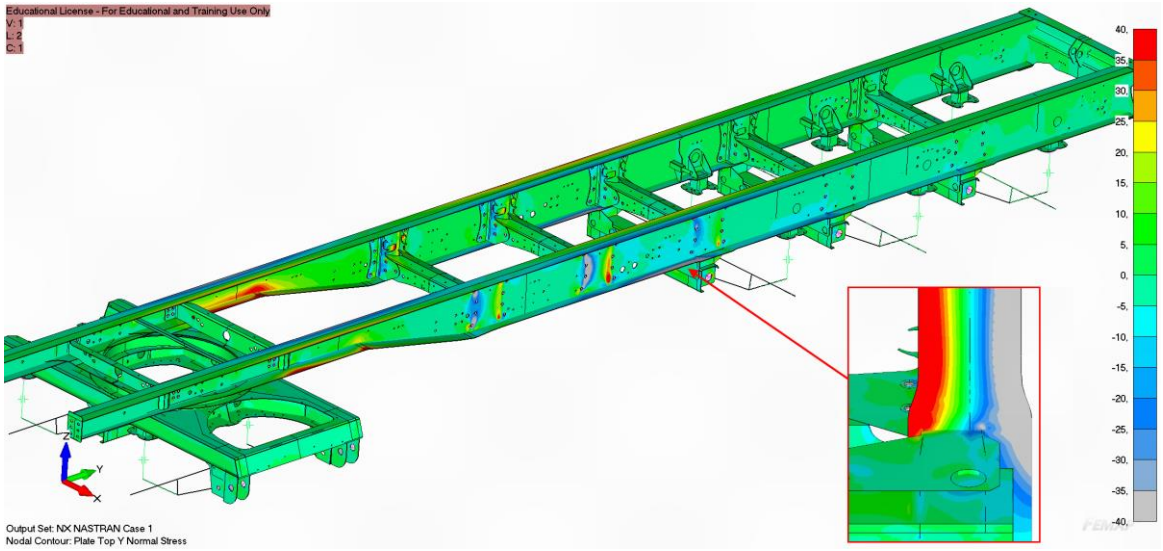

Figure 30. Side load, plate top y normal stress [MPa].

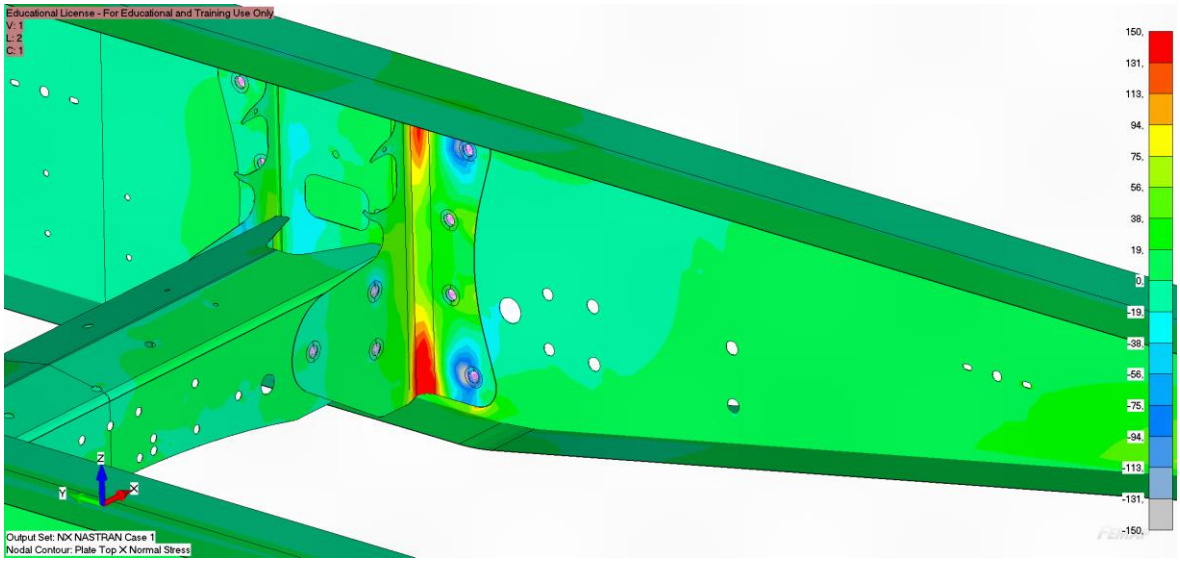

Figure 31. Side load at first transversal beam, plate top x normal stress [MPa].

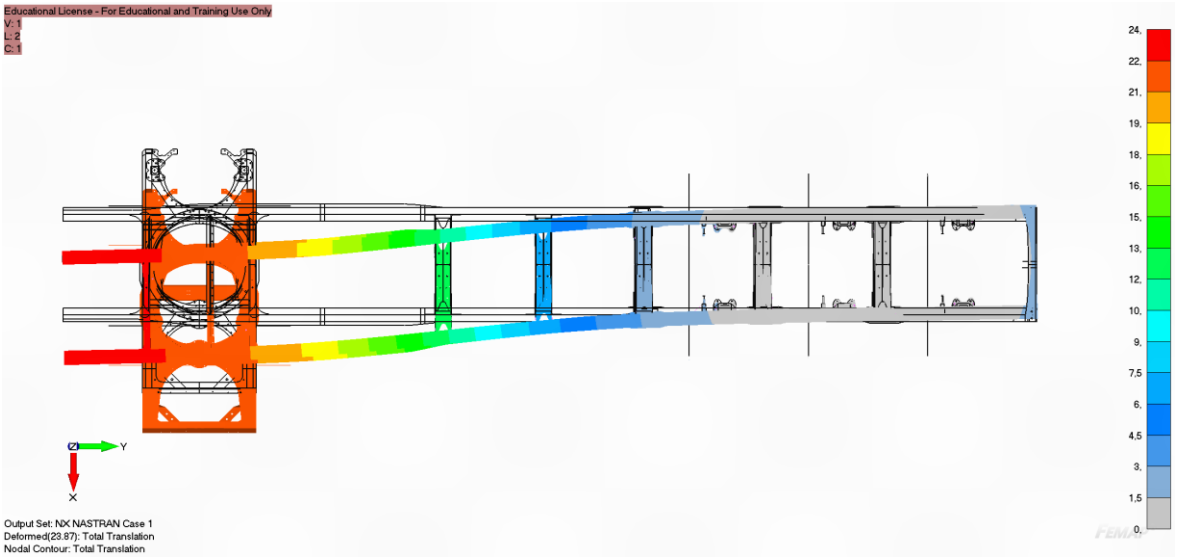

Figure 32. Side load deflection [mm].

4.3 Fatigue strength with 4R-method

For reference the lifetime of the weld was also calculated by Hot Spot-method for both measuring points. The measuring data represents an average day and presumably average usage is five days a week. This gives 260 working days in a year. With this assumption lifetime for SG1A is 1 year 6 months and SG1B 7 years and 3 months.

The residual stresses were measured from the test specimen for lifetime calculation by 4R-method and these are presented in table 8.

Table 8. Measured residual stresses.

Measuring line	Distance	MPa	(+/-)
A	0	-43	104,3
A	4,8	74	138,4
A	15	214	19,1
B	0	17	24
B	4,8	51	24,6
B	15	70	9,3

As in the chapter 3.4 was presented the most critical weld toe's radius was 0.12 mm which was used in the 4R-calculation. With this information calculated lifetime for SG1A was 2 years and 3 months and SG1B 5 years and 2 months.

4.4 FAT-class test

The FAT-class test was calculated by ENS-model to last 122 100 cycles. The weld residual stress measurements and weld's 3d-scan results are presented in chapters 3.4 and 4.3 The result from the test was 181 716 cycles when the flange cracked through whole width. In figures 33-36 the cycles aren't correct as the measuring equipment miscalculated. From these figures can be seen that measuring line A with strain gauges 1 and 2 started to fail first. Both strain gauges' max-min strain values are presented with delta strain values.

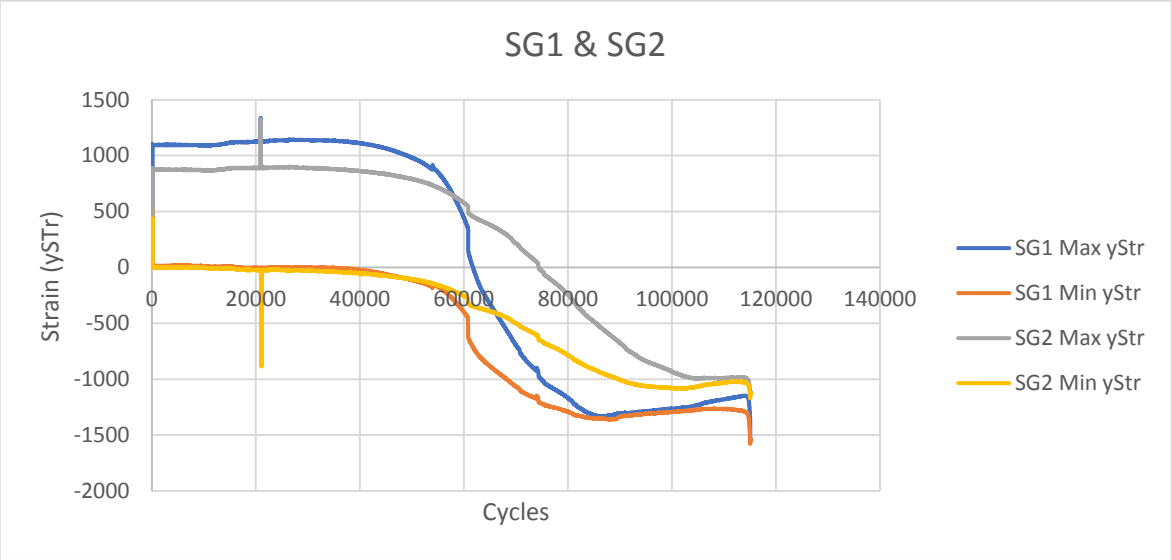

Figure 33. SG1 and SG2.

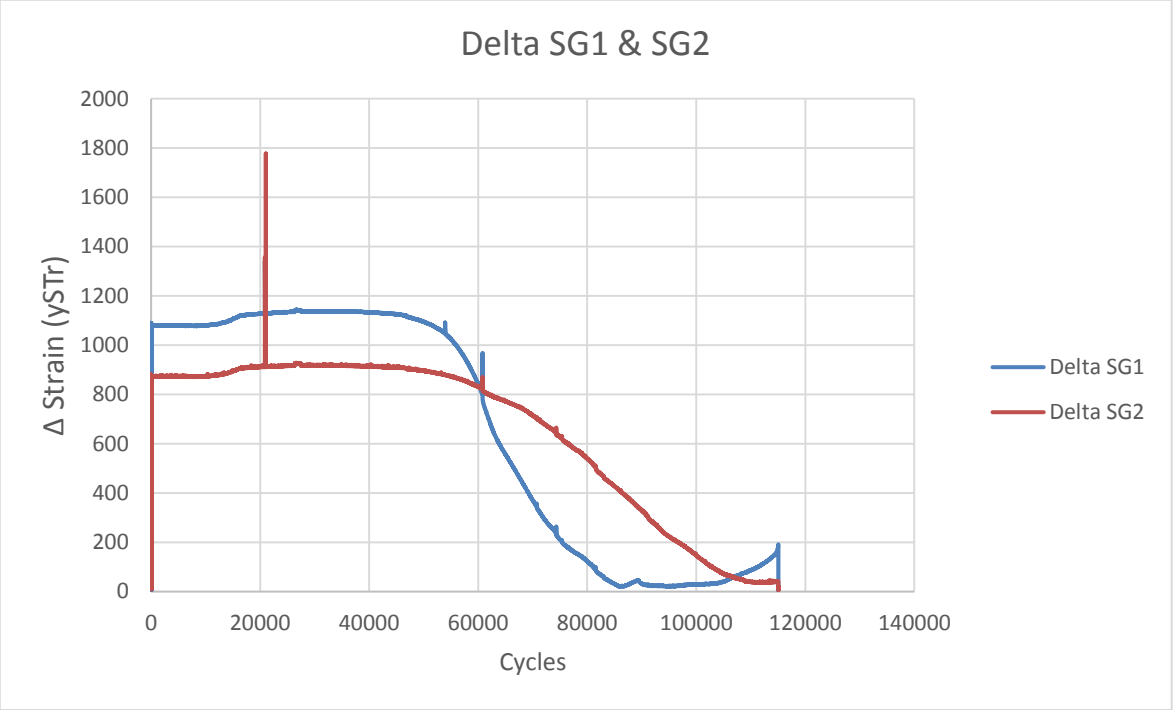

Figure 34. Delta strains SG1 and SG2.

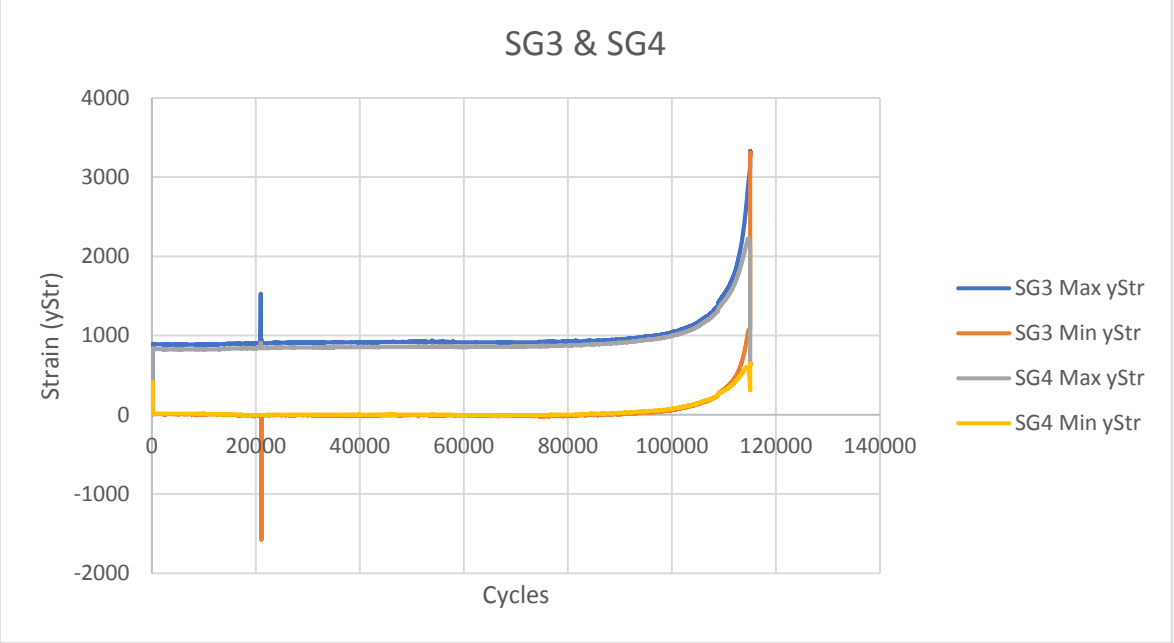

Figure 35. SG3 and SG4.

Figure 36. Delta strain valuesSG3 and SG4.

These strain gauges can be seen in figure 37.

Figure 37. Strain gauge positions.

The measured nominal stress amplitude from bending was 170 MPa which is close to the ENS-model's 160 MPa. With nominal stress amplitude and lifetime FAT-class can be calculated with equation (16).

$$N_f = \left(\frac{FAT}{\Delta\sigma}\right)^3 * 2 * 10^6 \quad (16)$$

The result is FAT 76 which is higher than the weld connection-based value of 63 from IIW standard. The actual test set up is shown in figure 38.

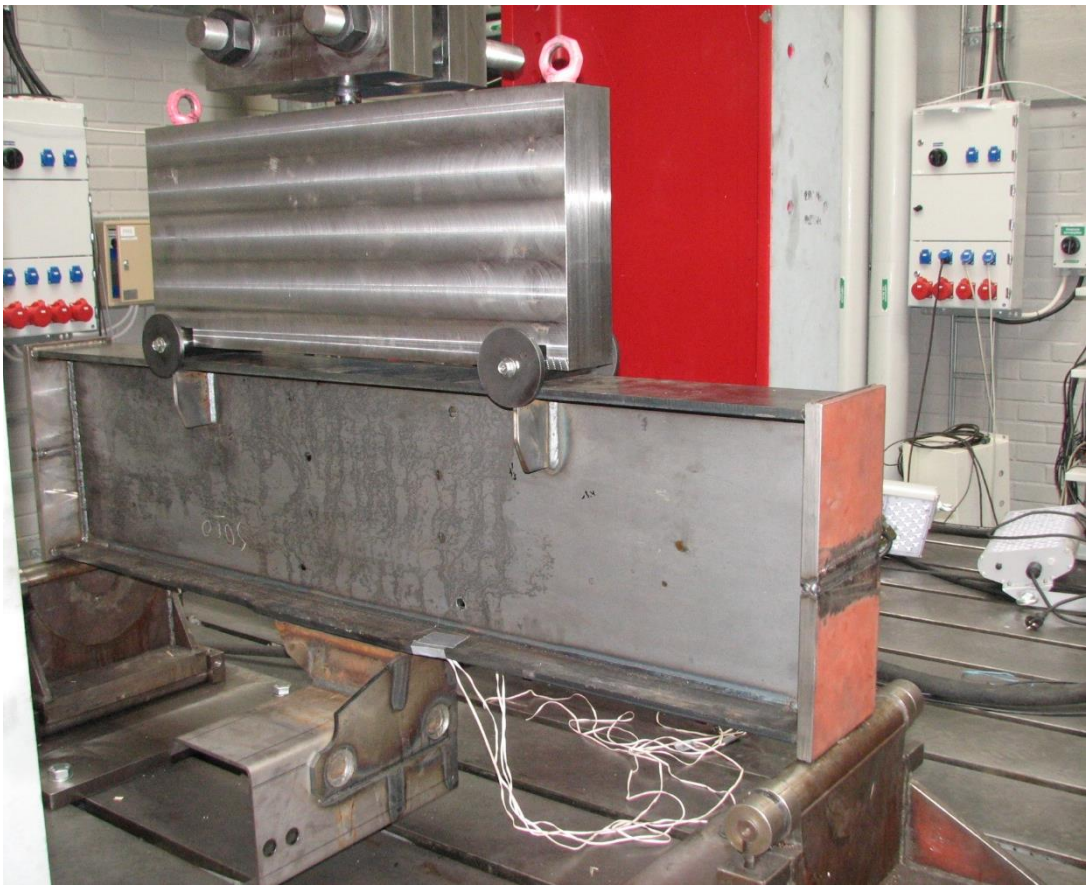

Figure 38. Test set up.

The main failure cracked the whole flange as the test stopped when deformation exceeded the limit value. There was also cracks at bracing plates' tips, but these didn't affect to the test result. The main failure occurred at weld toe, but secondary crack was also in the weld's root side. This didn't reach the whole width of the flange. These main failures are presented in figures 39 and 40.

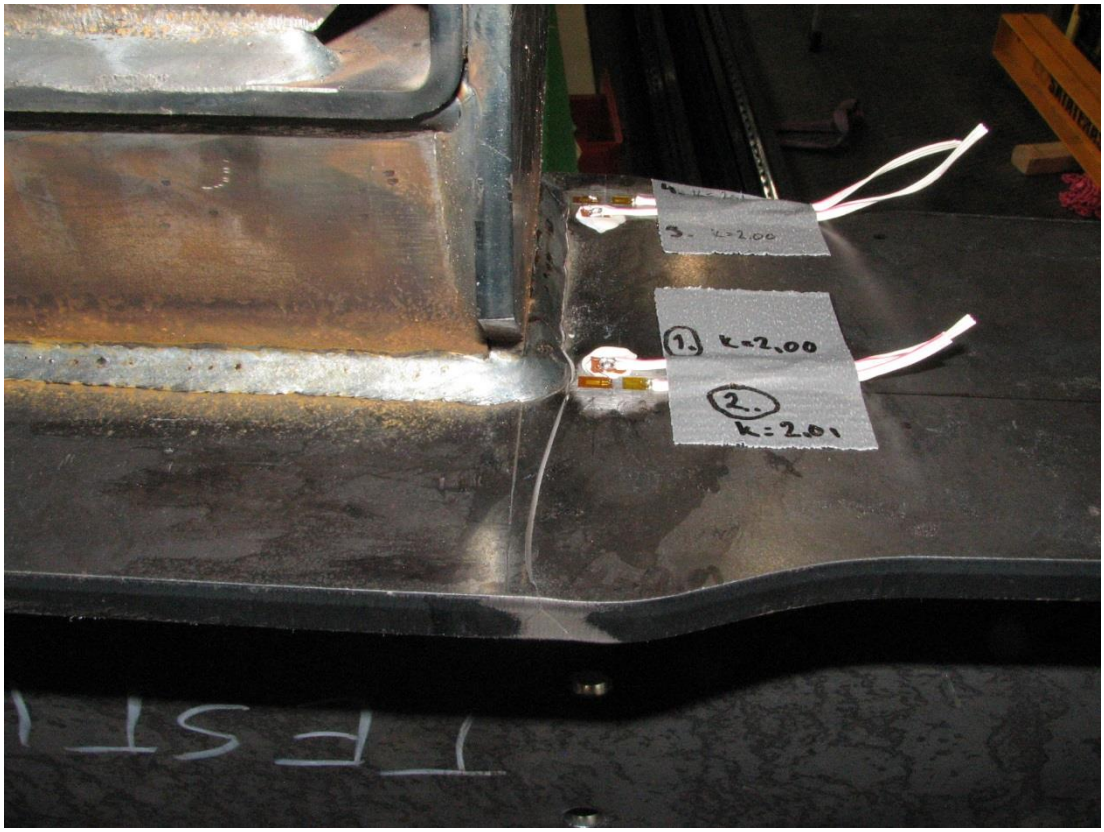

Figure 39. Weld toe and root crack.

Figure 40. Weld toe crack.

5 DISCUSSION

The strain gauge measurements' results varied more to FE-models' results as expected, but partly those are caused by factors that couldn't be replicated or modelled as accurately such as weight distribution, chassis' and tires' behavior under load and how it factored in measurements that trailer was already used. Still FE-model resulted good enough information about where the highest stresses were concentrated and served its' purpose. The strain gauge measurements were a success as the controlled and continuous measurements gave a lot of information of dynamic behavior in controlled measurements and overall view of the stresses with different road types in continuous measurements.

Fatigue lifetime calculations were in the end on the conservative side as the smallest weld toe radius was taken to the calculations and ENS-model which wasn't right on top of the stress hot spots. Also, the test specimen was especially made for this thus its' quality could have been different from the strain gauge measurement trailer depending on the manufacturing tolerances. The residual stress measurements were difficult to one side and that resulted a great variance which also affected to the lifetime results.

The designing of FAT-class test included the whole test setup and was tested in FE-models. This meant designing the test specimen and pressing tools such way that the failure will happen in the right spot. To ensure this the test specimen was reinforced at the pressing areas and right amount of force was calculated according to FE-models results. These measures led to a successful test and the failure occurred in the wanted weld toe. As the lifetime result was greater than anticipated the strength of the weld was adequate and high strength steel appeared to be a good choice for this kind of structure. In this case weld post treatment wouldn't be necessary because the failure is easier to spot from the weld toe than from the root side

For further development there are many things that can be done. One of the major ones that affected to the FE-models results is to study the chassis' behavior to get better understanding of it and thus better results. This could lead to FEM used more in designing for companies such as Jyki where it hasn't been used. Other thing could be optimizing the frame's structure

based on the measurements and do more measurements for verifying and getting new data to comprehend frame’s loadings more profoundly.

6 CONCLUSION

The purpose for this thesis was to identify global maximum forces and local stress peak areas in Jyki's timber trailer frame. At first FE-models were made to define where the highest stresses were located and how the frame behaved under load. These results gave the foundation to design strain gauge placement and measurements. Measurements were divided in three parts: static with and without cargo, controlled measurements and continuous measurement. Based on the continuous measurement fatigue lifetime was calculated for the most critical weld joint. The same weld joint was taken as test specimen to measure factors to fatigue lifetime calculation and to perform a FAT-class test.

The fatigue analyzes by 4R -method was applied for SG1A and SG1B which were placed for hotspot-distance from the weld toe. The truck was assumed to be operational 24 hours five times a week which resulted 260 days. With this assumption 4R-method resulted lifetimes of 2 years and 3 months for SG1A and 5 years and 2 months for SG1B. For comparison Hot Spot-method was also used and it resulted lifetimes of 1 year and 6 months for SG1A and 7 years and 3 months for SG1B. These were calculated with the smallest weld toe radius of 0.12 mm. This weld toe radius was measured from the test specimen and not from the actual trailer frame that was used for strain gauge measurements.

The FAT-class test was designed for the same weld as the 4R-method calculations were performed. Both the test specimen and the pressing tools were designed with FE-models which gave the needed specifications for the pressing width and force. The goal was to have weld failure approximately at 100 000 cycles. With ENS-calculations from the FE-model the failure was expected to occur at 122 100 cycles as the FAT-class for it was 63. At the actual test the failure occurred after 188 716 cycles which resulted 76 FAT-class for the weld. The failure originated from the weld toe as designed and went through the whole flange. Secondary failures were from weld root and tips of the reinforcement plates welds.

.

REFERENCES

6.6.2013. Valtioneuvoston asetus ajoneuvojen käytöstä tiellä annetun asetuksen muuttamisesta. [Cited 15.8.2018] Available: https://www.finlex.fi/fi/laki/alkup/2013/20130407#Pid1923449

Ahola, A. 2018. 4R-method presentation. Lecture material Steel Structures II. [Referenced 15.3.2019].

Ahola, A. Nykänen, T & Björk, T. 2017. Effect of loading type on the fatigue strength of asymmetric and symmetric transverse non-load carrying attachments. Fatigue & Fracture of Engineering Materials & Structures. 2016. Pp. 670-682.

HBM. 2018. Strain Measurement Basics. [HBM www-page]. [Cited 10.6.2018]. Available: https://www.hbm.com/en/6896/strain-measurement-basics/

Hobbacher, A. 2014. Recommendations for fatigue design of welded joints and components. IIW-document XIII-2460/XV-1440-13.

Kyowa. 2014. What's a strain gage? Introduction to strain gages. [web document]. Released 22.1.2014. [Cited 10.6.2018] Available: https://www.kyowa-ei.co.jp/english/products/gages/pdf/whats.pdf

Nykänen, T. & Björk, T. 2015. A new proposal for assessment of the fatigue strength of steel butt-welded joints improved by peening (HFMI) under constant amplitude tensile loading. Fatigue & Fracture of Engineering Materials & Structures. 2016. Pp. 566-582.

SSAB. 2018. Strenx 650 MC. [SSAB www-page]. [Referenced 8.8.2018]. Available: http://www.ssab.fi/tuotteet/brandit/strenx/tuotteet/strenx-650-mc

SSAB. 2018. Strenx 700 MC+. [SSAB www-page]. [Referenced 8.8.2018]. Available: https://www.ssab.fi/tuotteet/brandit/strenx/tuotteet/strenx-700-mc-plus

Appendix I

Measurement plan

Phase number	Instance	Specification	Explanation	Cargo load [t]	Repetitions	Estimated time of work cycle	Situation
1	Calibration						
2	Static measurements						
2.1		Full cargo, two log piles		35	1	15 min	OK, 25.7.2018
3	Single events						
3.1		Driving slowly over transversal obstacle, full cargo, both tires	75 mm high obstacle, 5 km/h	35	3	5 min	OK, 25.7.2018
3.2		Driving rapidly over transversal obstacle, full cargo, both tires	75 mm high obstacle, 15 km/h	35	3	5 min	OK, 25.7.2018
3.3		Driving slowly over transversal obstacle, full cargo, right side tires	75 mm high obstacle, 5 km/h	35	3	5 min	OK, 25.7.2018
3.4		Driving rapidly over transversal obstacle, full cargo, right side tires	75 mm high obstaclee, 15 km/h	35	3	5 min	OK, 25.7.2018
3.5		Driving over higher transversal obstacle, left side tires, full cargo	90 mm high obstacle, 5 km/h		3		OK, 25.7.2018
3.6		Turn with higher speed on paved yard, full cargo	Turn with speed of 30 km/h	35	2/direction	5 min	OK, 25.7.2018
3.7		Full turn from stationary position, full cargo	Turn from 90 degree angle	35	2/direction	5 min	OK, 25.7.2018
3.8		Full turn in motion, full cargo, last axel down	8-turn		2/direction	5 min	OK, 25.7.2018
3.9		Full turn in motion, full cargo, last axel up	8-turn		2/direction	5 min	OK, 25.7.2018
3.10		Full turn from stationary position, without cargo	Turn from 90 degree angle		2/direction	5 min	OK, 25.7.2018
3.11		Driving slowly over transversal obstacle, without cargo, both tires	75 mm high obstacle, 5 km/h		3	5 min	OK, 25.7.2018
3.12		Driving rapidly over transversal obstacle, without cargo, both tires	75 mm high obstacle, 15 km/h		3	5 min	OK, 25.7.2018
3.13		Driving slowly over transversal obstacle, without cargo, right side tires	75 mm high obstacle, 5 km/h		3	5 min	OK, 25.7.2018
3.14		Driving rapidly over transversal obstacle, without cargo, right side tires	75 mm high obstacle, 15 km/h		3	5 min	OK, 25.7.2018
4	Continuous event						
4.1		Forrest truck road without cargo				8h	OK, 23- 24.7.2018
4.2		Forrest truck road with full cargo	Full cargo, two log piles	35		8h	OK, 23- 24.7.2018
4.3		Dirt road without cargo				8h	OK, 23- 24.7.2018
4.4		Dirt road with full cargo	Full cargo, two log piles	35		8h	OK, 23- 24.7.2018
4.5		Main road without cargo				8h	OK, 23- 24.7.2018
4.6		Main road with full cargo	Full cargo, two log piles	35		8h	OK, 23- 24.7.2018

Strain gauge positions Appendix II

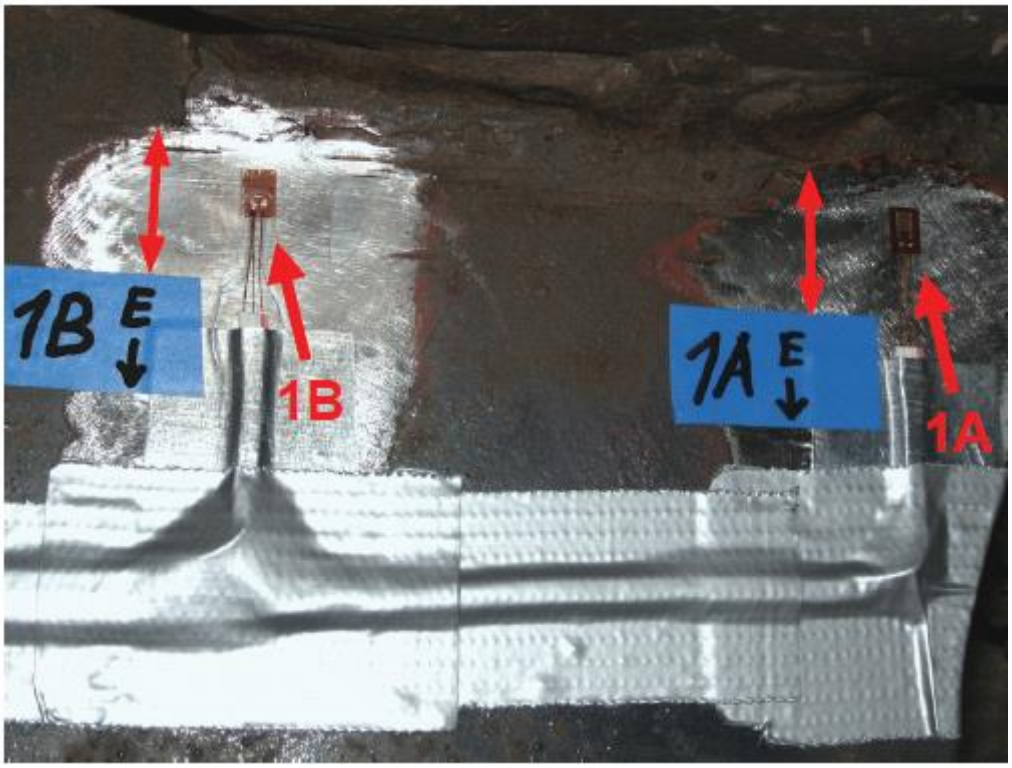
1B E
1B
1A E
1A


2A
2B
E

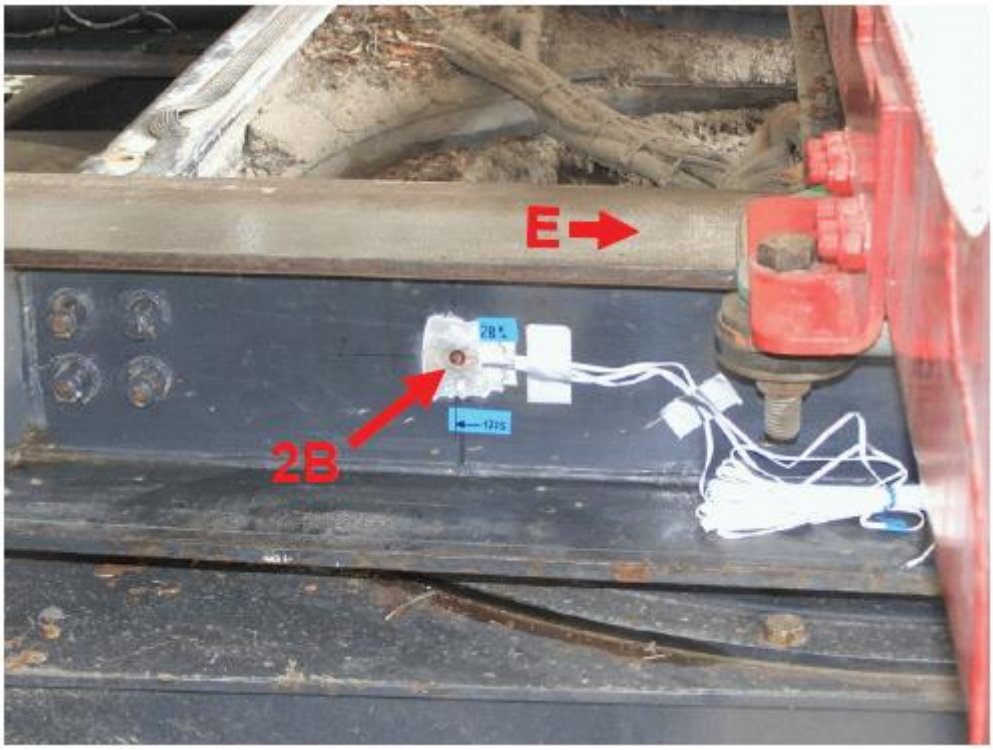
E
2B

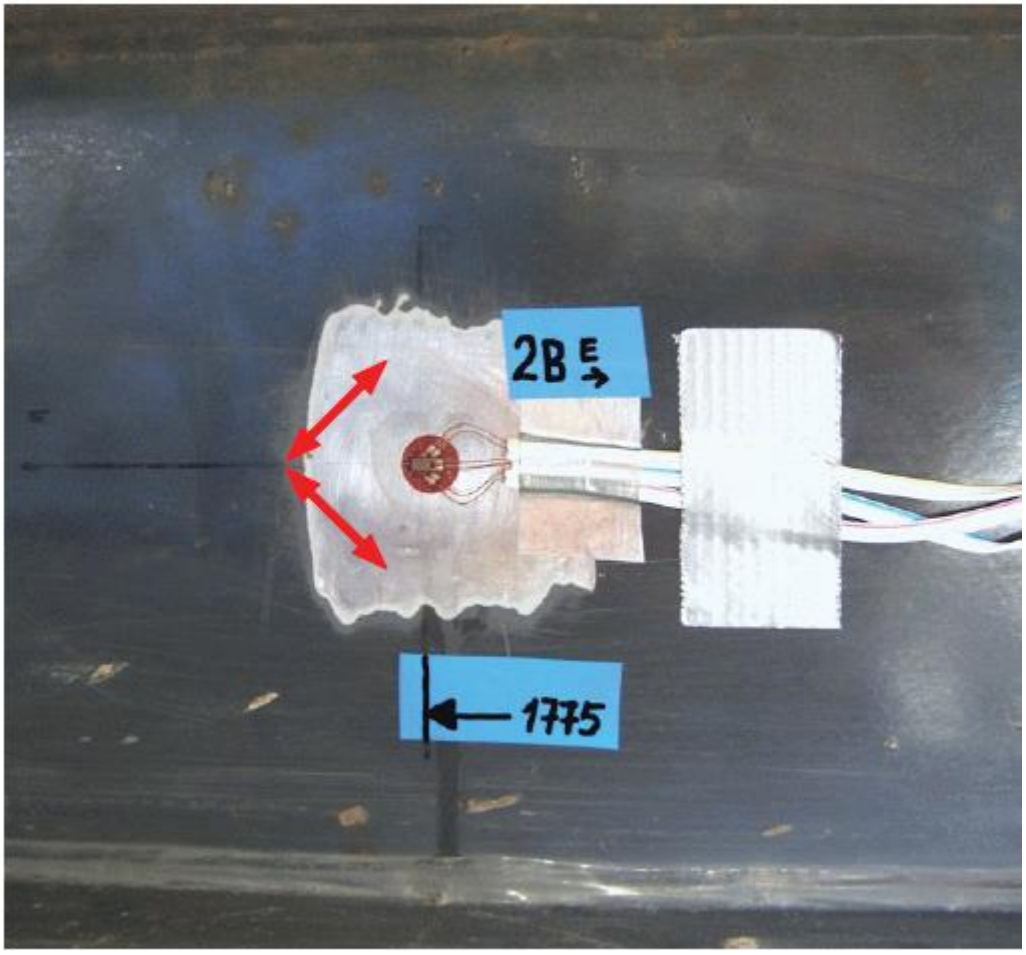
2B E
1775

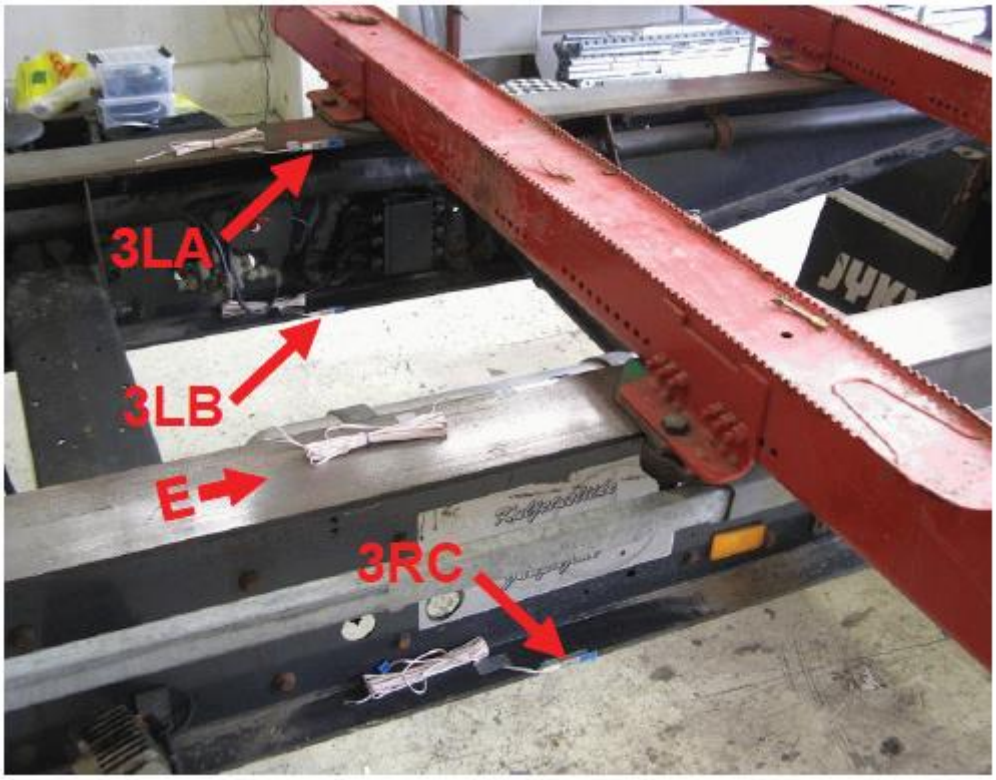
3LA
3LB
E
3RC

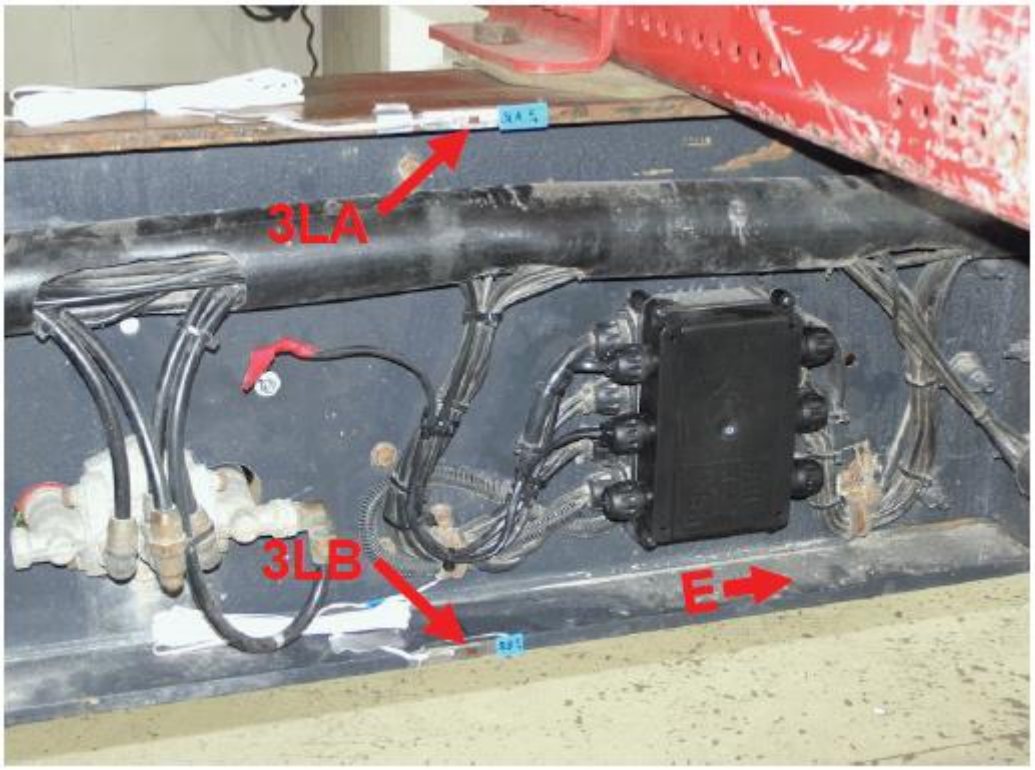
3LA
3LB
E

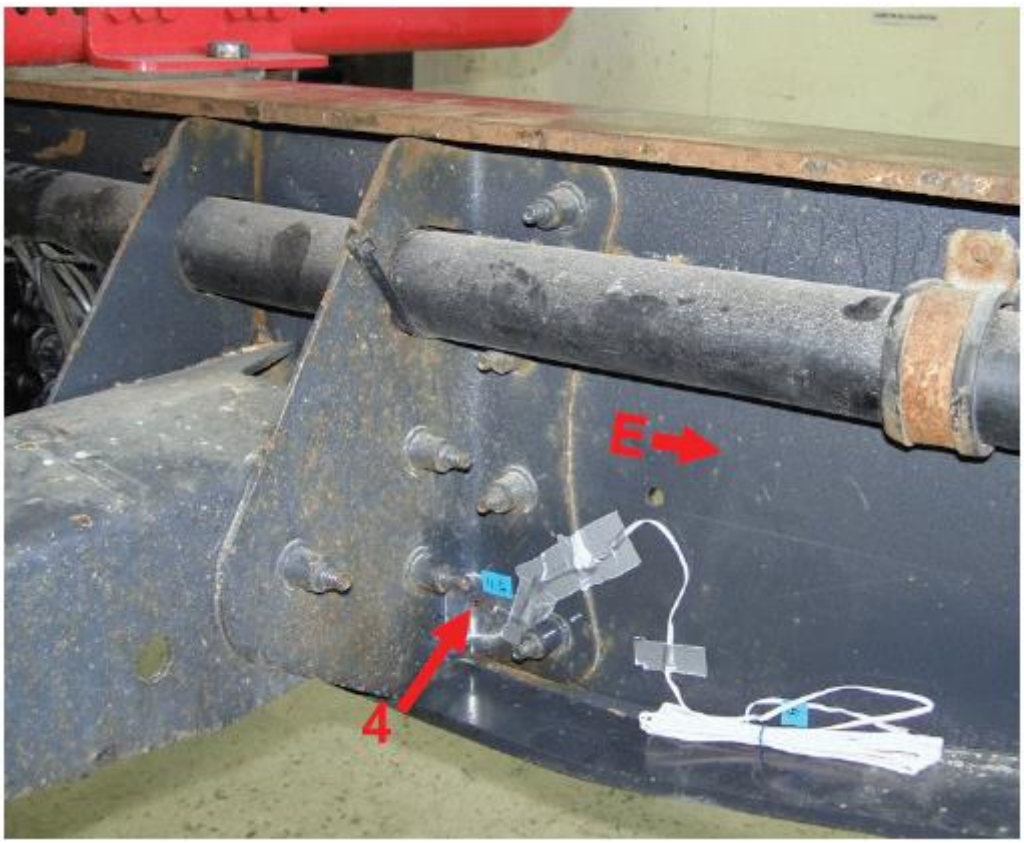
E
4

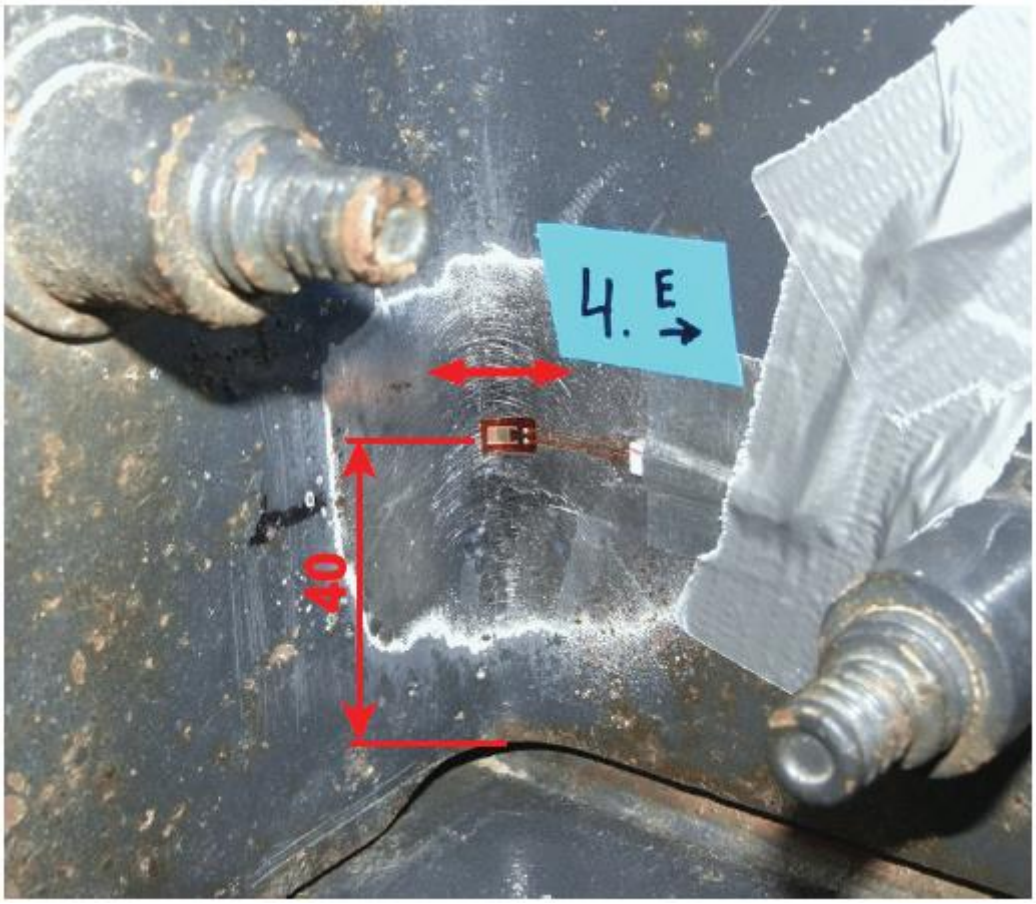
4. E
10

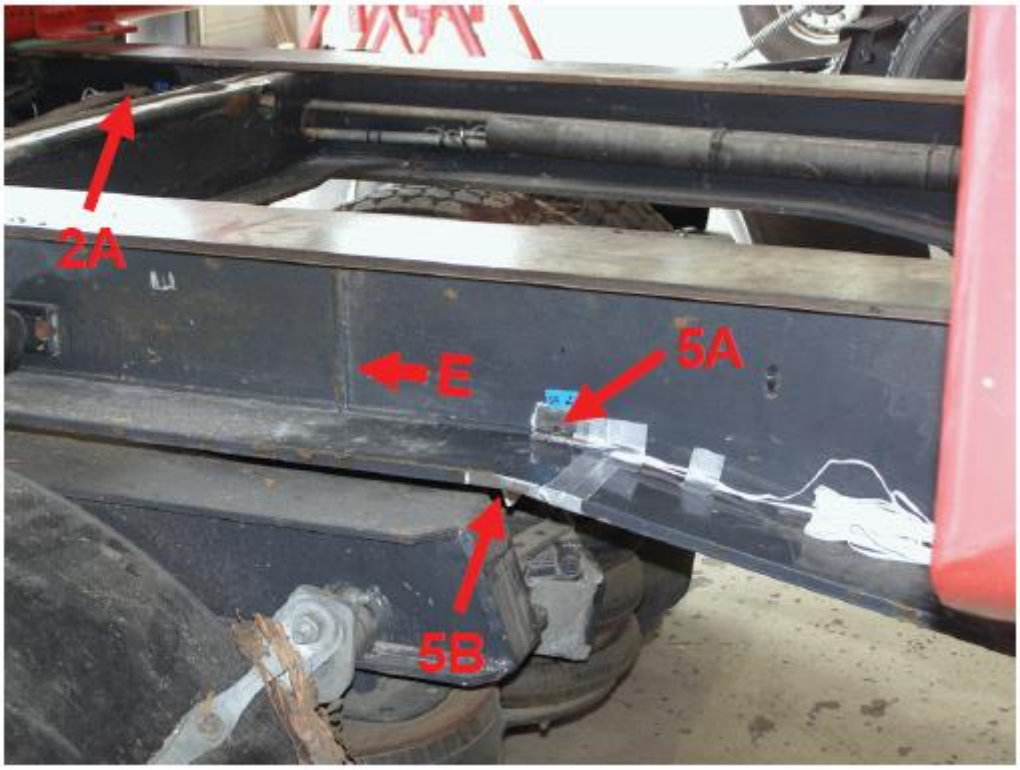
2A
E
5A
5B

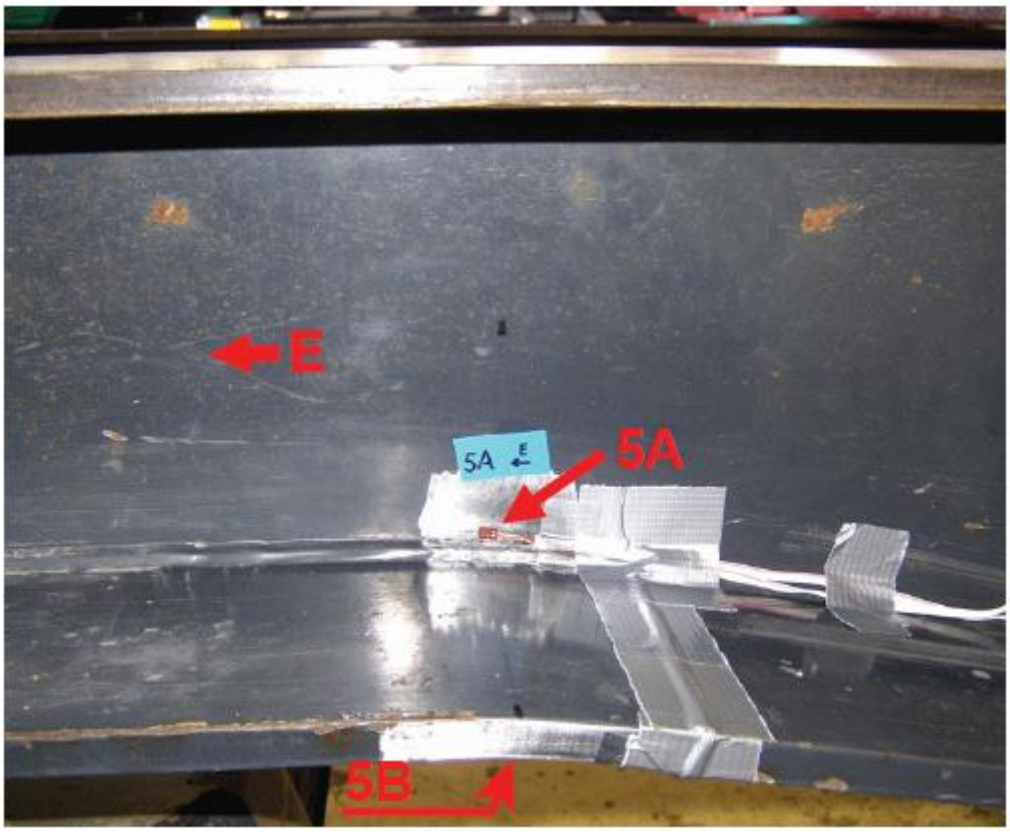
E
5A
5A
5B

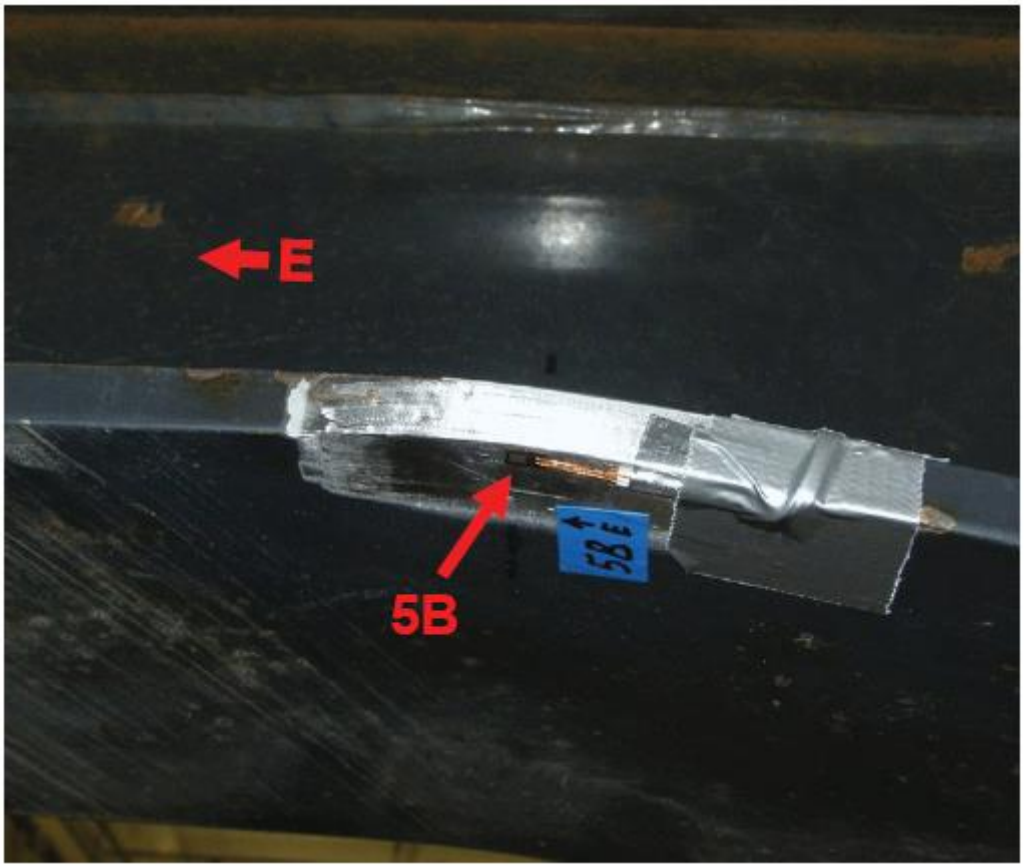
E
5B
5B E


ACC_E

SG 1B

$\sigma_1 := 48.81 \quad \sigma_2 := -11.5$

$\sigma_m := \frac{\sigma_1 + \sigma_2}{2} = 18.655 \quad \sigma_b := \frac{\sigma_1 - \sigma_2}{2} = 30.155 \quad R_1 := \frac{\sigma_2}{\sigma_1} = -0.236$

$\sigma_{1.ens} := 110.18 \quad \sigma_{2.ens} := -9.5 \quad R_1 := \frac{\sigma_{2.ens}}{\sigma_{1.ens}} = -0.086$

$\sigma_{m.ens} := \frac{\sigma_{1.ens} + \sigma_{2.ens}}{2} = 50.34 \quad \sigma_{b.ens} := \frac{\sigma_{1.ens} - \sigma_{2.ens}}{2} = 59.84$

$K_{t.m} := \frac{\sigma_{m.ens}}{\sigma_m} = 2.698 \quad K_{t.b} := \frac{\sigma_{b.ens}}{\sigma_b} = 1.984$

$\sigma_1 := 25.6 \quad \sigma_2 := -6.1$

$\sigma_m := \frac{\sigma_1 + \sigma_2}{2} = 9.75 \quad \sigma_b := \frac{\sigma_1 - \sigma_2}{2} = 15.85 \quad R_1 := \frac{\sigma_2}{\sigma_1} = -0.238$

$\sigma_{1.ens} := 57.8 \quad \sigma_{2.ens} := -5 \quad R_1 := \frac{\sigma_{2.ens}}{\sigma_{1.ens}} = -0.087$

$\sigma_{m.ens} := \frac{\sigma_{1.ens} + \sigma_{2.ens}}{2} = 26.4 \quad \sigma_{b.ens} := \frac{\sigma_{1.ens} - \sigma_{2.ens}}{2} = 31.4$

$K_{t.m} := \frac{\sigma_{m.ens}}{\sigma_m} = 2.708 \quad K_{t.b} := \frac{\sigma_{b.ens}}{\sigma_b} = 1.981 \quad R_1 := \frac{\sigma_{2.ens}}{\sigma_{1.ens}} = -0.087$

$\sigma_1 := 72.1 \quad \sigma_2 := -16.9$

$\sigma_m := \frac{\sigma_1 + \sigma_2}{2} = 27.6 \quad \sigma_b := \frac{\sigma_1 - \sigma_2}{2} = 44.5 \quad R_1 := \frac{\sigma_2}{\sigma_1} = -0.234$

$\sigma_{1.ens} := 57.8 \quad \sigma_{2.ens} := -5 \quad R_1 := \frac{\sigma_{2.ens}}{\sigma_{1.ens}} = -0.087$

$\sigma_{m.ens} := \frac{\sigma_{1.ens} + \sigma_{2.ens}}{2} = 26.4 \quad \sigma_{b.ens} := \frac{\sigma_{1.ens} - \sigma_{2.ens}}{2} = 31.4$

$K_{t.m} := \frac{\sigma_{m.ens}}{\sigma_m} = 0.957 \quad K_{t.b} := \frac{\sigma_{b.ens}}{\sigma_b} = 0.706 \quad R_1 := \frac{\sigma_{2.ens}}{\sigma_{1.ens}} = -0.087$

$sigma := 1.67 \cdot 40.1 - 0.67 \cdot 27.1 = 48.81$

$\frac{40.1}{27.1} = 1.48$

$\frac{\sigma_{1.ens}}{sigma} = 2.257$

$sigma := 1.67 \cdot 21 - 0.67 \cdot 14.2 = 25.556$

$\frac{21}{14.2} = 1.479$

$\frac{\sigma_{1.ens}}{sigma} = 2.262$

$sigma := 1.67 \cdot 59.2 - 0.67 \cdot 40 = 72.064$

$\frac{59.2}{40} = 1.48$

Sivuveto SG 1B

$\sigma_1 := -47.734 \quad \sigma_2 := -10.56$

$\sigma_m := \frac{\sigma_1 + \sigma_2}{2} = -29.147 \quad \sigma_b := \frac{\sigma_1 - \sigma_2}{2} = -18.587 \quad R_1 := \frac{\sigma_2}{\sigma_1} = 0.221$

$\sigma_{1.ens} := -109.63 \quad \sigma_{2.ens} := -12.2 \quad R_1 := \frac{\sigma_{2.ens}}{\sigma_{1.ens}} = 0.111$

$\sigma_{m.ens} := \frac{\sigma_{1.ens} + \sigma_{2.ens}}{2} = -60.915 \quad \sigma_{b.ens} := \frac{\sigma_{1.ens} - \sigma_{2.ens}}{2} = -48.715$

$K_{t.m} := \frac{\sigma_{m.ens}}{\sigma_m} = 2.09 \quad K_{t.b} := \frac{\sigma_{b.ens}}{\sigma_b} = 2.621$

$sigma := 1.67 \cdot -40.9 - 0.67 \cdot -30.7 = -47.734$

$\frac{40.9}{30.7} = 1.332 \quad \frac{37.44}{53.3} = 0.702$

$\frac{\sigma_{1.ens}}{sigma} = 2.297$

SG 1A

$\sigma_1 := 34.1 \quad \sigma_2 := -5.5$

$\sigma_m := \frac{\sigma_1 + \sigma_2}{2} = 14.3 \quad \sigma_b := \frac{\sigma_1 - \sigma_2}{2} = 19.8 \quad R_1 := \frac{\sigma_2}{\sigma_1} = -0.161$

$\sigma_{1.ens} := 77.34 \quad \sigma_{2.ens} := -5.74 \quad R_1 := \frac{\sigma_{2.ens}}{\sigma_{1.ens}} = -0.074$

$\sigma_{m.ens} := \frac{\sigma_{1.ens} + \sigma_{2.ens}}{2} = 35.8 \quad \sigma_{b.ens} := \frac{\sigma_{1.ens} - \sigma_{2.ens}}{2} = 41.54$

$K_{t.m} := \frac{\sigma_{m.ens}}{\sigma_m} = 2.503 \quad K_{t.b} := \frac{\sigma_{b.ens}}{\sigma_b} = 2.098$

$sigma := 1.67 \cdot 31.5 - 0.67 \cdot 27.7 = 34.046$

$\frac{31.5}{27.7} = 1.137 \quad \frac{34.046}{31.5} = 1.081 \quad \frac{30.5}{31.5} = 0.968$

$\frac{\sigma_{1.ens}}{sigma} = 2.272 \quad \frac{\sigma_{1.ens}}{31.5} = 2.455$

$\sigma_1 := 18.1 \quad \sigma_2 := -2.9$

$\sigma_m := \frac{\sigma_1 + \sigma_2}{2} = 7.6 \quad \sigma_b := \frac{\sigma_1 - \sigma_2}{2} = 10.5 \quad R_1 := \frac{\sigma_2}{\sigma_1} = -0.16$

$\sigma_{1.ens} := 40.7 \quad \sigma_{2.ens} := -3.03$

$\sigma_{m.ens} := \frac{\sigma_{1.ens} + \sigma_{2.ens}}{2} = 18.835 \quad \sigma_{b.ens} := \frac{\sigma_{1.ens} - \sigma_{2.ens}}{2} = 21.865$

$K_{t.m} := \frac{\sigma_{m.ens}}{\sigma_m} = 2.478 \quad K_{t.b} := \frac{\sigma_{b.ens}}{\sigma_b} = 2.082 \quad R_1 := \frac{\sigma_{2.ens}}{\sigma_{1.ens}} = -0.074$

$sigma := 1.67 \cdot 16.7 - 0.67 \cdot 14.6 = 18.107$

$\frac{16.7}{14.6} = 1.144 \quad \frac{18.107}{16.7} = 1.084 \quad \frac{16.042}{16.7} = 0.961$

$\frac{\sigma_{1.ens}}{sigma} = 2.248 \quad \frac{\sigma_{1.ens}}{16.7} = 2.437$

$\sigma_1 := 51.1 \qquad \sigma_2 := -8.1$

$\sigma_m := \frac{\sigma_1 + \sigma_2}{2} = 21.5 \qquad \sigma_b := \frac{\sigma_1 - \sigma_2}{2} = 29.6 \qquad R_1 := \frac{\sigma_2}{\sigma_1} = -0.159$

$\sigma_{1.ens} := 114.02 \qquad \sigma_{2.ens} := -8.4$

$\sigma_{m.ens} := \frac{\sigma_{1.ens} + \sigma_{2.ens}}{2} = 52.81 \qquad \sigma_{b.ens} := \frac{\sigma_{1.ens} - \sigma_{2.ens}}{2} = 61.21$

$K_{t.m} := \frac{\sigma_{m.ens}}{\sigma_m} = 2.456 \qquad K_{t.b} := \frac{\sigma_{b.ens}}{\sigma_b} = 2.068 \qquad R_1 := \frac{\sigma_{2.ens}}{\sigma_{1.ens}} = -0.074$

$sigma := 1.67 \cdot 47 - 0.67 \cdot 40.9 = 51.087$

$\frac{47}{40.9} = 1.149 \qquad \frac{51.087}{47} = 1.087$

$\frac{\sigma_{1.ens}}{sigma} = 2.232$

Sivuveto SG 1A

$\sigma_1 := 56.85 \qquad \sigma_2 := 37.4$

$\sigma_m := \frac{\sigma_1 + \sigma_2}{2} = 47.125 \qquad \sigma_b := \frac{\sigma_1 - \sigma_2}{2} = 9.725 \qquad R_1 := \frac{\sigma_2}{\sigma_1} = 0.658$

$\sigma_{1.ens} := 118.2 \qquad \sigma_{2.ens} := 38.92 \qquad R_1 := \frac{\sigma_{2.ens}}{\sigma_{1.ens}} = 0.329$

$\sigma_{m.ens} := \frac{\sigma_{1.ens} + \sigma_{2.ens}}{2} = 78.56 \qquad \sigma_{b.ens} := \frac{\sigma_{1.ens} - \sigma_{2.ens}}{2} = 39.64$

$K_{t.m} := \frac{\sigma_{m.ens}}{\sigma_m} = 1.667 \qquad K_{t.b} := \frac{\sigma_{b.ens}}{\sigma_b} = 4.076$

$sigma := 1.67 \cdot 53.3 - 0.67 \cdot 48 = 56.851$

$\frac{53.3}{48} = 1.11$

$\frac{\sigma_{1.ens}}{sigma} = 2.079 \qquad \frac{\sigma_{1.ens}}{53.3} = 2.218$

$\sigma_1 := 76 \qquad \sigma_2 := 49.8$

$\sigma_m := \frac{\sigma_1 + \sigma_2}{2} = 62.9 \qquad \sigma_b := \frac{\sigma_1 - \sigma_2}{2} = 13.1 \qquad R_1 := \frac{\sigma_2}{\sigma_1} = 0.655$

$\sigma_{1.ens} := 161.7 \qquad \sigma_{2.ens} := 52.3 \qquad R_1 := \frac{\sigma_{2.ens}}{\sigma_{1.ens}} = 0.323$

$\sigma_{m.ens} := \frac{\sigma_{1.ens} + \sigma_{2.ens}}{2} = 107 \qquad \sigma_{b.ens} := \frac{\sigma_{1.ens} - \sigma_{2.ens}}{2} = 54.7$

$K_{t.m} := \frac{\sigma_{m.ens}}{\sigma_m} = 1.701 \qquad K_{t.b} := \frac{\sigma_{b.ens}}{\sigma_b} = 4.176$

$sigma := 1.67 \cdot 71.23 - 0.67 \cdot 64.13 = 75.987$

$\frac{53.3}{48} = 1.11$

$\frac{\sigma_{1.ens}}{sigma} = 2.128 \qquad \frac{\sigma_{1.ens}}{71.23} = 2.27$

$$n := \frac{160}{1 - 0.05} = 168.421 \qquad n_2 := n - 3.60525 = 164.816$$

$$\sigma_{max} := \frac{\sigma}{210000} + \left(\frac{\sigma}{1485}\right)^{\frac{1}{0.15}} - \frac{(n_2)^2}{210000 \cdot \sigma} = 0 \text{ solve} \rightarrow 164.77056662783722728$$

$$\sigma_{\Delta} := \frac{\sigma}{210000} + 2 \cdot \left(\frac{\sigma}{2 \cdot 1485}\right)^{\frac{1}{0.15}} - \frac{160^2}{210000 \cdot \sigma} = 0 \text{ solve} \rightarrow 159.99926780188411413$$

$$\sigma_{min} := \sigma_{max} - \sigma_{\Delta} = 4.771 \qquad R_{local} := \frac{\sigma_{min}}{\sigma_{max}} \text{ float}, 6 \rightarrow 0.0289572$$

$$N_f := \frac{\left(\sqrt{1 - R_{local}}\right)^{5.85} \cdot 10^{20.83}}{\sigma_{\Delta}^{5.85}} = 7.917 \times 10^7$$

$$N_{block} := \frac{0.2}{\left(\frac{2}{N_f}\right)} = 7.917 \times 10^6$$